BOUNDARY ELEMENT METHODS

We will study potential and linear elasticity problems which represent a wide range of problems in applied mathematics, physics and engineering. Some of the physical situations which have models involving these equations are: Steady-state heat conduction problems, torsion problems in solid mechanics, diffusion flow in porous media, incompressible inviscid fluid flow, electrostatic potential problems, Newtonian potentials, and magnetostatics. We will introduce the boundary element method for two-dimensional steady-state potential and elastic problems. In a very general form, this method starts by dividing the boundary of the region into finitely many elements (hence the name boundary element method, or BEM). This article is condensed from Kythe (1995).

Potential Problems

1. Laplace Equation. We will solve the mixed Laplace boundary value problem

$$\nabla^2 u = 0, \quad u = u_0 \text{ on } C_1, \quad \frac{\partial u}{\partial n} \equiv q = q_0 \text{ on } C_2, \tag{1.1}$$

where $C = C_1 \cup C_2$ is the boundary of a region R. Since $-\nabla^2 u^* = \delta(\mathbf{x}, \mathbf{x}')$, where $u^*(\infty) = 0$, and δ denotes the Dirac delta function, the potential boundary value problem with a concentrated charge acting at a point $\mathbf{x}' = \mathbf{x}_i \equiv i$ can be written as

$$\nabla^2 u^* = -\delta(i); \quad u^* = u^*(\mathbf{x}, \mathbf{x}'). \tag{1.2}$$

The solution of this problem is called the fundamental solution for the potential problem. In view of the translation property of the delta function,

$$0 = \iint_R u\big[\nabla^2 u^* + \delta(i)\big]\, dx\, dy = \iint_R u\nabla^2 u^*\, dx\, dy + u(i), \tag{1.3}$$

where $u(i)$ denotes the value of the unknown potential u at the point i where the charge is applied. Note that we are writing $u(i)$ for $u(x_i)$, where x_i is the source point, thus $r = |x_j - x_i|$. Now, the weak variational form for the boundary value problem (1.1) becomes

$$\begin{aligned} 0 &= \iint_R \big(\nabla^2 u\big) w\, dx\, dy \\ &= -\iint_R \Big(\frac{\partial u}{\partial x}\frac{\partial w}{\partial x} + \frac{\partial u}{\partial y}\frac{\partial w}{\partial y}\Big)\, dx\, dy + \int_C w\frac{\partial u}{\partial n}\, ds, \\ &= \iint_R u\nabla^2 w\, dx\, dy - \int_C u\frac{\partial w}{\partial n}\, ds + \int_C w\frac{\partial u}{\partial n}\, ds. \end{aligned}$$

Thus,

$$-\iint_R u\nabla^2 w\,dx\,dy = \int_C w\frac{\partial u}{\partial n}\,ds - \int_C u\frac{\partial w}{\partial n}\,ds. \tag{1.4}$$

Since $u = u_0$ on C_1 and $\partial u/\partial n \equiv q = q_0$ on C_2, we replace w by u^* (and hence, q by q^*) in (1.4), and from (1.3) and (1.4) we obtain

$$u(i) = \int_{C_1} u^* q\,ds + \int_{C_2} u^* q_0\,ds - \int_{C_1} u_0 q^*\,ds - \int_{C_2} uq^*\,ds, \tag{1.5}$$

where $q^* = \partial u^*/\partial n$. Recall that for an isotropic two-dimensional region, the fundamental solution is given by $u^* = \dfrac{1}{2\pi}\log\dfrac{1}{r}$, where $r = |\mathbf{x} - \mathbf{x}'|$ is the distance from the point of application of the delta function to the point under consideration. The symmetric form of the two-dimensional Laplace equation in polar cylindrical coordinates is

$$\frac{\partial^2 u^*}{\partial r^2} + \frac{1}{r}\frac{\partial u^*}{\partial r} = -\delta(i). \tag{1.6}$$

Substituting the above value of u^* into (1.6) yields $\delta(i) = 0$ for $r \neq 0$. Thus, this equation is satisfied for any $r \neq 0$. Since at $r = 0$ the fundamental solution u^* has a logarithmic singularity, we proceed as follows: Integrate on a circle K surrounding the boundary point i where the charge is applied. This gives

$$\iint_R \nabla^2 u^*\,dx\,dy = -\iint_R \delta(i)\,dx\,dy = -1. \tag{1.7}$$

To show that the first integral in (1.7) is also equal to -1, we find that

$$\iint_R \nabla^2 u^*\,dx\,dy = \int_K q^*\,ds = \int_K \frac{\partial u^*}{\partial r}\,ds. \tag{1.8}$$

Substituting the above fundamental solution u^* into (1.8) we get

$$\int_K \frac{\partial u^*}{\partial r}\,ds = \frac{1}{2\pi}\int_0^{2\pi}\Big(-\frac{1}{r}\Big)\,r\,d\theta = -1. \tag{1.9}$$

Note that this result (-1) is independent of r. Thus, the left side goes to -1 as $r \to 0$.

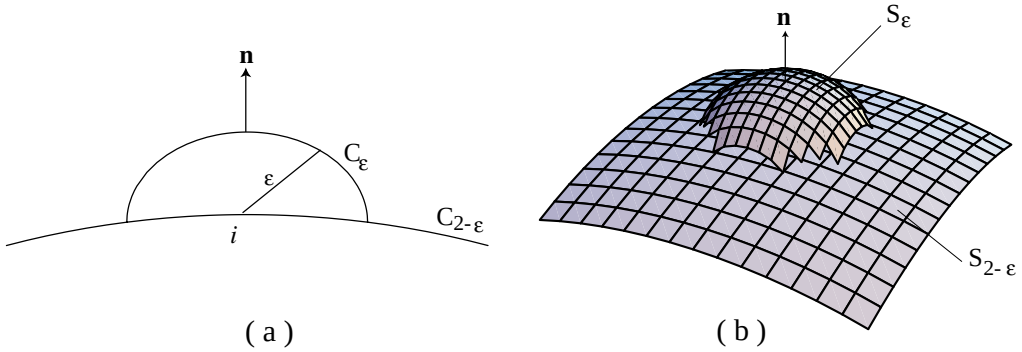

Fig. 1.1.

Eq (1.5), where $u(i)$ is the value of the unknown potential u at the point i of the application of the charge, is valid at any point of the region. However, in order to solve it by the boundary element method, we will formulate it on the boundary. One of the simplest ways to consider a semicircle C_ε of radius ε on the boundary of a two-dimensional region R, as in Fig. 1.1(a). Assume that the boundary point i is at the center of this semicircle. As $\varepsilon \to 0$, the semicircle will reduce to the boundary point i. Further, assume that the boundary C of the region R is smooth, and that $C = C_1 \cup C_2$. Let the boundary point i be on the C_2 portion of C (similar considerations apply if it is on C_1). Divide the boundary C_2 into two parts: C_ε and $C_{2-\varepsilon}$. Then

$$\int_{C_2} uq^*\,ds = \int_{C_2-\varepsilon} uq^*\,ds + \int_{C_\varepsilon} uq^*\,ds. \tag{1.10}$$

Substitute the fundamental solution u^* into the second integral on the right side and take the limit. This integral becomes

$$\lim_{\varepsilon\to 0}\int_{C_\varepsilon} uq^*\,ds = \lim_{\varepsilon\to 0}\int_{C_\varepsilon} u\Big(-\frac{1}{2\pi\varepsilon}\Big)\,ds = -\lim_{\varepsilon\to 0}\frac{u}{2\pi\varepsilon}\int_{C_\varepsilon} ds = -\frac{u}{2}, \tag{1.11}$$

where $\int_{C_\varepsilon} ds = \pi\varepsilon$ (circumference of the semicircle). Now since ε is zero, the boundary $C_{2-\varepsilon}$ again becomes C_2. Also, note that the right side of (1.5) gives

$$\lim_{\varepsilon\to 0}\int_{C_\varepsilon} qu^*\,ds = \lim_{\varepsilon\to 0}\frac{q}{2\pi}\ln\frac{1}{\varepsilon}\int_{C_\varepsilon} ds = -\frac{q}{2}\lim_{\varepsilon\to 0}\varepsilon\,\ln\varepsilon = 0. \tag{1.12}$$

Thus, this limiting process does not introduce any new terms in (1.5).

Now, substituting (1.11) into (1.5), we obtain the following two-dimensional BI Eq for a node i on the boundary C_2:

$$\frac{u(i)}{2} + \int_{C_1} u_0 q^*\,ds + \int_{C_2} uq^*\,ds = \int_{C_1} u^* q\,ds + \int_{C_2} u^* q_0\,ds. \tag{1.13}$$

We will obtain the same result if we consider the point i on the C_1 portion of the boundary instead of C_2.

In the three-dimensional case, consider the Laplace equation $\nabla^2 u = 0$ with the boundary conditions $u = u_0$ on S_1 and $q = q_0$ on S_2, where $S = S_1 \cup S_2$ is the boundary (surface) of an isotropic region. We will take a hemisphere S_ε (of radius ε and center at i, see Fig. 1.1(b)) such that $S_2 = S_{2-\varepsilon} + S_\varepsilon$. Then Eq (1.10) becomes

$$\iint_{S_2} uq^*\,dS = \iint_{S_{2-\varepsilon}} uq^*\,dS + \iint_{S_\varepsilon} uq^*\,dS. \tag{1.10a}$$

We substitute the fundamental solution $u^* = \dfrac{1}{4\pi\,|\mathbf{x}-\mathbf{x}'|}$ into the second integral in (1.10a). Then

$$\lim_{\varepsilon\to 0}\iint_{S_\varepsilon} uq^*\,dS = \lim_{\varepsilon\to 0}\iint_{S_\varepsilon} u\Big(-\frac{1}{4\pi\varepsilon^2}\Big)\,dS = -\lim_{\varepsilon\to 0}\frac{u}{4\pi\varepsilon^2}\iint_{S_\varepsilon} dS = -\frac{u}{2}, \tag{1.11a}$$

where $\iint_{S_\varepsilon} dS = 2\pi\varepsilon^2$ (surface area of the hemisphere). In this limit process the boundary $S_{2-\varepsilon}$ becomes S_2, and

$$\lim_{\varepsilon\to 0}\iint_{S_\varepsilon} qu^*\,dS = \lim_{\varepsilon\to 0}\frac{q}{2\pi\varepsilon}\iint_{C_\varepsilon} dS = \lim_{\varepsilon\to 0}\frac{q}{2\pi\varepsilon}\left(2\pi\varepsilon^2\right) = 0. \tag{1.12a}$$

Thus, the three-dimensional BI Eq for a node i on the boundary S_2 is given by

$$\frac{u(i)}{2} + \iint_{S_1} u_0 q^*\,dS + \iint_{S_2} uq^*\,dS = \iint_{S_1} u^* q\,dS + \iint_{S_2} u^* q_0\,dS. \tag{1.13a}$$

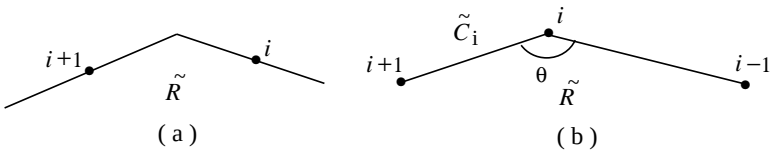

Fig. 1.2.

In general, BI Eq (1.13) or (1.13a) can be written as

$$c(i)u(i) + \int_C uq^*\,ds = \int_C u^* q\,ds, \quad C = C_1 \cup C_2, \tag{1.14}$$

or

$$c(i)u(i) + \iint_S uq^*\,dS = \iint_S u^* q\,dS, \quad S = S_1 \cup S_2, \tag{1.14a}$$

respectively, under the essential boundary conditions $u = u_0$ on C_1 (or on S_1) and the natural boundary condition $\partial u/\partial n \equiv q = q_0$ on C_2 (or on S_2), where in two-dimensional case

$$c(i) = \begin{cases} 0 & \text{if } i \text{ is outside } R \cup C \\ 1 & \text{if } i \text{ is inside } R \\ 1/2 & \text{if } i \text{ is on a smooth portion of } C \\ \theta/2\pi & \text{if } i \text{ is at a corner node,} \end{cases} \tag{1.15}$$

θ being the internal angle (in radian) at the corner at node i (see Fig. 1.2(b)). In Fig. 1.2(a), the value of $c(i) = 1/2$. The coefficient $c(i)$ can be evaluated analytically, or by considering different cases of the values of potential and flux 'before' and 'after' a corner node (see §2.3). In the case of a three-dimensional region, $c(i)$ has the same values relative to the boundary surface S except at a corner node on S where it has the value $\theta/4\pi$, θ being the solid (internal) angle at that node.

2. Boundary Elements. We discretize (partition) the smooth boundary C of a two-dimen sional region R into N segments $C_j,\ j = 1, \ldots, N$ (Fig. 2.1). The chords joining the partition points are called the $boundary\ elements$ and will be denoted by $\tilde{C}_j, j = 1, \ldots, N$; the partition points are called the $extreme\ points$ of the boundary elements. The discretization of the boundary produces, in general, an approximate region $\tilde{R}$ and an approximate (polygonal) boundary $\tilde{C} = \cup_{j=1}^{N}\tilde{C}_j$. The

portion between the boundary C and the approximate boundary $\tilde{C}$ will produce a discretization error. The choice of boundary elements should always minimize the discretization error. If the boundary conditions are mixed, i.e., if the essential and natural boundary conditions are applied on two portions C_1 and C_2 ($C = C_1 \cup C_2$), the two points common to these portions are taken as extreme points. In the case of zero discretization error, we will have $\tilde{R} = R$ and $\tilde{C} = C$.

The points where both known and unknown values of u and q are considered according to the prescribed boundary conditions are called $nodes$. Three types of nodes are explained in Fig. 2.2:

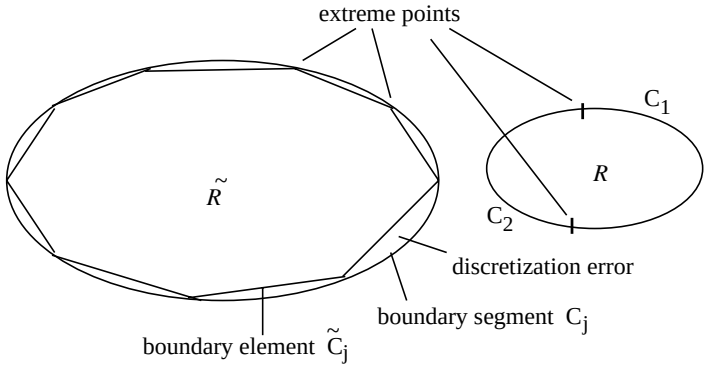

Fig. 2.1.

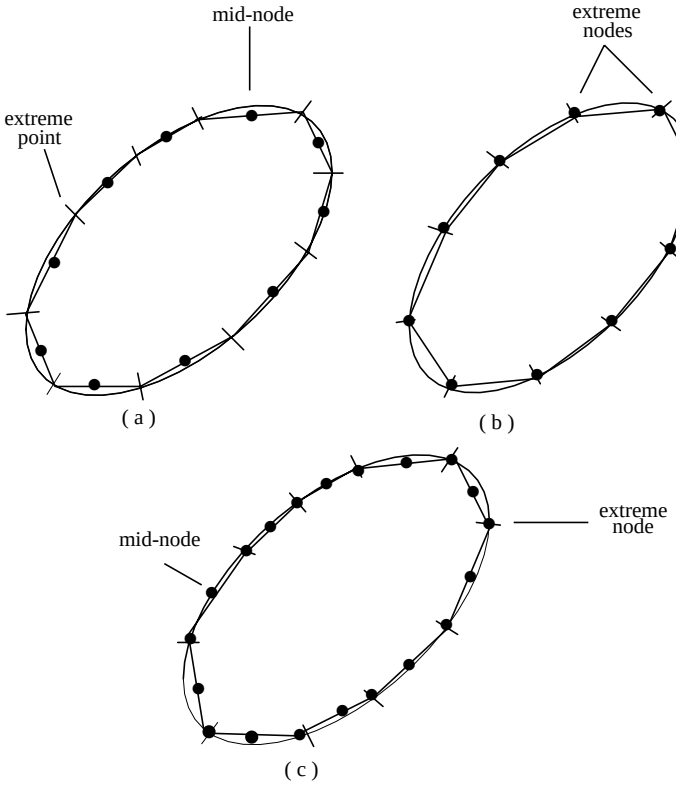

Fig. 2.2. Elements, Mid-nodes, and extreme nodes.

1. Constant elements have mid-nodes, which are taken at the midpoint of each element, as in Fig. 2.2.(a);

2. Linear elements have extreme nodes, which are at the intersection between two elements, as in Fig. 2.2.(b); and

3. Quadratic elements have both mid- and extreme nodes, as in Fig. 2.2(c).

2.1. Constant Elements. Let the boundary C of the region R be smooth, and let it be discretized into N elements, of which N_1 elements belong to C_1 and N_2 to C_2. This discretization produces an approximate region $\tilde{R}$ and an approximate boundary $\tilde{C}$. Assume that the values of u and $q \equiv \partial u/\partial n$ are constant on each element and equal to the value at the mid-node of the respective element. Eq (1.14) for a given node i becomes in the discretized form

$$\frac{u(i)}{2} + \sum_{j=1}^{N} u_j \int_{\tilde{C}_j} q^* \, ds = \sum_{j=1}^{N} q_j \int_{\tilde{C}_j} u^* \, ds, \tag{2.1}$$

where $q^* \equiv \partial u^*/\partial n$. This BE Eq applies to a particular node i. Note that the terms with $\int_{\tilde{C}_j}$ relate to the node i with segment j over which the integral is evaluated. Denote the integrals $\int_{\tilde{C}_j} q^* \, ds$ on the left side of (2.1) by $\hat{H}_{ij}$, and the integrals $\int_{\tilde{C}_j} u^* \, ds$ on the right side by G_{ij}. Then Eq (2.1) becomes

$$\frac{u(i)}{2} + \sum_{j=1}^{N} u_j \hat{H}_{ij} = \sum_{j=1}^{N} q_j G_{ij}. \tag{2.2}$$

The integrals $\hat{H}_{ij}$ and G_{ij} are easy to evaluate for the constant element case. However, for higher order elements they are more difficult to evaluate analytically and will be computed by using the Gauss-Legendre quadrature rules (see §3.2.2 in the Handbook).

Eq (2.2) relates the value of u at the mid-node i with the value of u and q at all the nodes on the boundary including i. If we write Eq (2.2) for each mid-node i, we get a system of N equations:

$$\sum_{j=1}^{N} H_{ij} u_j = \sum_{j=1}^{N} G_{ij} q_j, \tag{2.3}$$

where

$$H_{ij} = \begin{cases} \hat{H}_{ij} & \text{for } i \neq j \\ \hat{H}_{ij} + \dfrac{1}{2} & \text{for } i = j. \end{cases} \tag{2.4}$$

Eq (2.2) can be written as in matrix form as

$$HU = GQ. \tag{2.5}$$

Note that $N = N_1 + N_2$, and that the N_1 values of u and N_2 values of q are known (prescribed). So we have a set of N unknowns in (2.5).

The terms H_{ii} include the coefficients $c(i)$ ($= 1/2$ for smooth boundary, see Fig. 1.2(a)). These terms are evaluated under the condition that when a uniform potential u is applied over the entire finite region the value of $q = \partial u/\partial n$ must be zero. Then (2.5) implies that

$$HI = 0, \tag{2.6}$$

where I is the unit column vector. Eq (2.6) means that the sum of all elements of H in a row should be zero. Thus, the values of the diagonal coefficients can be easily computed once all the off-diagonal coefficients are known, i.e.,

$$H_{ii} = -\sum_{\substack{j=1 \\ i \neq j}}^{N} H_{ij}, \quad i = 1, \cdots, N. \tag{2.7}$$

Let us denote the N_2 unknown values of u by $\hat{u}$ and the N_1 values of q by $\hat{q}$. We can reorder Eq (2.5) such that all the unknowns (N_2 of $\hat{u}$ and N_1 of $\hat{q}$) are on the right side. Then Eq (2.5) can be written as

$$AX = F, \tag{2.8}$$

where X is the vector of unknowns u and q. Hence, we can determine all the values of u and q on the entire boundary $\tilde{C}$ from (2.8). Once this is done, we can compute the value of u at any interior point by using (1.5) which in the discretized form is

$$u(i) = \sum_{j=1}^{N} q_j G_{ij} - \sum_{j=1}^{N} u_j \hat{H}_{ij}. \tag{2.9}$$

The internal fluxes $q_x = \partial u/\partial x$ and $q_y = \partial u/\partial y$ can be computed by differentiating (1.5); thus, at the node i

$$\begin{aligned} q_x(i) &= \int_{\tilde{C}} q \frac{\partial u^*}{\partial x}\, ds - \int_{\tilde{C}} u \frac{\partial q^*}{\partial x}\, ds, \\ &= \sum_{j=1}^{N} q_j \left(\int_{\tilde{C}_j} \frac{\partial u^*}{\partial x}\, ds \right) - \sum_{j=1}^{N} u_j \left(\int_{\tilde{C}_j} \frac{\partial q^*}{\partial x}\, ds \right), \end{aligned} \tag{2.10a}$$

$$\begin{aligned} q_y(i) &= \int_{\tilde{C}} q \frac{\partial u^*}{\partial y}\, ds - \int_{\tilde{C}} u \frac{\partial q^*}{\partial y}\, ds \\ &= \sum_{j=1}^{N} q_j \left(\int_{\tilde{C}_j} \frac{\partial u^*}{\partial y}\, ds \right) - \sum_{j=1}^{N} u_j \left(\int_{\tilde{C}_j} \frac{\partial q^*}{\partial y}\, ds \right), \end{aligned} \tag{2.10b}$$

where

$$\begin{aligned} \frac{\partial u^*}{\partial x} &= \frac{1}{2\pi} \frac{\partial}{\partial x} (-\ln r) = -\frac{1}{2\pi r} \frac{\partial r}{\partial x}, \\ \frac{\partial u^*}{\partial y} &= \frac{1}{2\pi} \frac{\partial}{\partial y} (-\ln r) = -\frac{1}{2\pi r} \frac{\partial r}{\partial y}, \\ \frac{\partial q^*}{\partial x} &= \frac{1}{2\pi} \left[\frac{1}{r} \left(\frac{\partial r}{\partial x} n_1 + \frac{\partial r}{\partial y} n_2 \right) \right], \\ \frac{\partial q^*}{\partial y} &= \frac{1}{2\pi} \left[\frac{1}{r} \left(\frac{\partial r}{\partial x} n_1 + \frac{\partial r}{\partial y} n_2 \right) \right], \end{aligned} \tag{2.11}$$

and n_1, n_2 are the components of the unit normal $\hat{\mathbf{n}}$. The integrals in (2.10) are evaluated numerically by the Gauss-Legendre quadrature. So also are the integrations for $\hat{H}_{ij}$ and G_{ij} done numerically by Gauss-Legendre quadrature for all elements $j \neq i$. For the node i, note that $\hat{H}_{ii} = 0$ (due to the orthogonality of $\mathbf{r}$ and $\hat{\mathbf{n}}$), and

$$G_{ii} = \int_{C_i} u^*\, ds = \frac{1}{2\pi} \int_{C_i} \ln\left(\frac{1}{r}\right) ds = \frac{L_i}{2\pi} \left[1 - \ln\left(\frac{L_i}{2}\right) \right], \tag{2.12}$$

where $L_i = \sqrt{(x_{i+1} - x_i)^2 + (y_{i+1} - y_i)^2}$ is the length of the element i (see Fig. 2.3.).

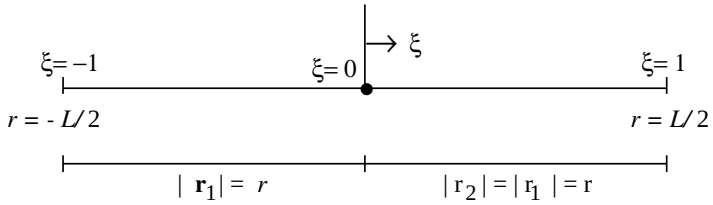

Fig. 2.3. A constant element.

For the derivation of (2.12), we take $r = \xi L_i/2$, so $r = 0$ at $\xi = 0$ and $r = \pm L_i/2$ at $\xi = \pm 1$. Then, since $\ln(1/r)$ has a logarithmic singularity at $r = \xi = 0$,

$$\begin{aligned} G_{ii} &= \frac{1}{2\pi} \int_{\tilde{C}_i} \ln(\frac{1}{r})\, ds = \frac{1}{2\pi}\, 2 \int_0^1 \ln\Big(\frac{2}{\xi L_i}\Big) \frac{L_i}{2}\, d\xi \\ &= \frac{L_i}{2\pi} \Big[\xi \ln \frac{2}{L_i} - \xi \ln \xi + \xi\Big]_0^1 \\ &= \frac{L_i}{2\pi} \Big[1 + \ln(\frac{2}{L_i})\Big], \end{aligned}$$

which gives (2.12).

Program Be1

For computer implementation in this case, the program Be1.c solves isotropic potential problems with constant u and q at the mid-nodes and computes them at the required interior points of the region. The input file is created in the format explained below. It can be named Be1.in, or any other name, not to exceed 10 characters including the extension which may be .in or .dat. The output file, named Be1.out, or any other name not to exceed 10 characters, can be typed (on screen), printed (hard copy), or used as input for graphics.

Dictionary of Variables:

`N`	Number of boundary elements (same as the number of mid-nodes in this case)
`L`	Number of interior points where the results are to be computed
`Code`	Indicator for the type of boundary conditions at the nodes. `Code`$= 0$: Only the value of u is known at the node. `Code`$= 1$: Only the value of q is known at the node.
`X`	x-coordinate of extreme-points.
`Y`	y-coordinate of extreme-points.
`Xm`	x-coordinate of mid-nodes.
`Xm(j)`	x-coordinate of mid-node j.
`Ym`	y-coordinate of mid-nodes.
`Ym(j)`	y-coordinate of mid-node j.

`G`	Matrix defined in (2.5). After the boundary conditions are imposed, the matrix A of (2.8) is stored in this location.
`H`	Matrix defined in (2.5).
`Bc(j)`	Prescribed values of boundary conditions for node j. If `Code`$= 0$, then `Bc(j)` contains prescribed values of u. If `Code`$= 1$, then `Bc(j)` contains prescribed values of q.
`F`	Right side vector in (2.8). After solution, the values of unknown u and q are returned in this location.
`Xi`	x-coordinate of the interior point where the value of u is required.
`Yi`	y-coordinate of the interior point where the value of u is required.
`u`	Vector of potential values at interior points.
`Dim`	Maximum dimension of the system of Eqs (2.5).
`Perp`	Perpendicular distance from the point (x_p, y_p) to the element j (Fig. 2.5a).
`Xg, Yg`	(x, y)-coordinates of Gauss points (nodes) ζ_i, $i = 1, 2, 3, 4$
`HL`	Half-length of the element $\tilde{C}_i$ $(= L_i/2)$.
`nx, ny`	n_x, n_y (components of the unit normal vector $\hat{\mathbf{n}}$).
`rx, ry, rn`	$r_{,x}, r_{,y}, r_{,n}$ (note that $r_{,n} = r_{,x}n_x + r_{,y}n_y$).

For the values Gauss-Legendre nodes and weights, see Table A.06 on this CD-R.

Input Format: The input file contains the data in the following order:

Entry #	Variable	Explanation
1	Title	Must enter problem title (max 80 chars).
2	`N`	Number of boundary elements.
3	`L`	Number of interior points where solution is to be computed.
next N-pairs	`X, Y`	x, y coordinates of extreme points (see Note below).
next N-pairs	`Code, Bc`	N-pairs of `Code` (0 or 1) and `Bc` at each mid-node, starting with node 1 and ending with node N.
next L-pairs	`Xi, Yi`	x and y coordinates of interior points where the solution is to be computed.

Note: The N-pairs of entries for the coordinates of the extreme points of boundary elements are read in counterclockwise order if the region R is interior to the boundary C, and in clockwise order if R is exterior to the boundary C. The convention is to traverse the boundary in such a manner that

the region R remains to the left.

The program Be1 calls the following functions: `Sys1, Quad1, Diag1, Inter1, and Solve`.

`Sys1` can be summarized by the following algorithm:

1. Compute the coordinates $(X_m, Y_m), m = 1, \cdots, N$, of the mid-nodes from the extreme nodes (x_j, y_j):

$$x_{n+1} = x_1,\ y_{n+1} = y_1 \quad \text{(see Fig. 2.4.);}$$
$$X_m = \frac{x_j + x_{j+1}}{2}, \quad Y_m = \frac{y_j + y_{j+1}}{2} \quad \text{for } j = 1 \text{ to } N.$$

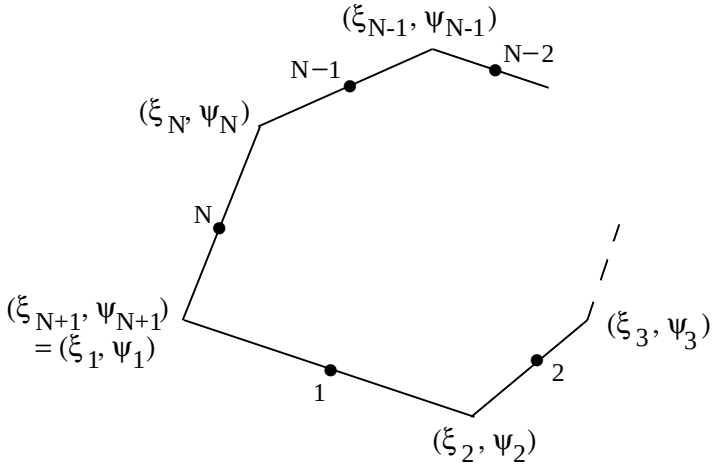

Fig. 2.4.

2. Compute the matrices H and G:

for $j = 1$ to N
for $k = 1$ to N
$j \neq k$: call `Quad1`
$j = k$: call `DIAG1`

3. Produce the matrix Eq (2.8) $F = AX$:

for $k = 1$ to N
if `Code`$(k) = 1$, then for $j = 1$ to N
`temp` $= G_{jk}$; $G_{jk} = -H_{jk}$; $H_{jk} = -$`temp` $= -G_{jk}$,

where `temp` is a temporary memory location. As a result, the matrix A is in location G; F is not yet evaluated, but all known terms are in the location of H and U. The location H contains both known G and H, and the location U contains both known U and Q.

4. Finally,

$$F_j = 0.0 \quad \text{for } j = 1 \text{ to } N$$
$$F_j = F_j + H_{jk} \cdot \texttt{Bc}_k \quad \text{for } k = 1 \text{ to } N.$$

The left side now stores F (all known values). The rearrangement of the system of equations to form the matrix A (now stored in `G`) and the left side vector F (stored as `F`) of Eq (2.8) is explained as follows: Suppose, Eq (2.4) (or in its matrix form (2.5)) is written, in the expanded form, as

$$\begin{array}{cc} & \texttt{Code } 0 \qquad \texttt{Code } 1 \\ H_{11}\hat{u}_1 + H_{12}\hat{u}_2 + H_{13}u_3 + \cdots + H_{1n}u_n = & G_{11}q_1 + G_{12}q_2 + G_{13}\hat{q}_3 + \cdots + G_{1n}\hat{q}_n \\ H_{21}\hat{u}_1 + H_{22}\hat{u}_2 + H_{23}u_3 + \cdots + H_{2n}u_n = & G_{21}q_1 + G_{22}q_2 + G_{23}\hat{q}_3 + \cdots + G_{2n}\hat{q}_n \\ \vdots & \\ H_{n1}\hat{u}_1 + H_{n2}\hat{u}_2 + H_{n3}u_3 + \cdots + H_{nn}u_n = & G_{n1}q_1 + G_{n2}q_2 + G_{n3}\hat{q}_3 + \cdots + G_{nn}\hat{q}_n, \end{array} \tag{2.13}$$

where $\hat{u}, \hat{q}$ denote the unknown values. In view of part 3 of the above algorithm, we note that G_{jk} is first stored in the location `temp`, then $-H_{jk}$ is moved to G_{jk}, and finally replace the values G_{jk}, stored at `temp`, to the location $-H_{jk}$. The result is the matrix equation (2.8), thus rendering the system (2.13) into the form

$$\begin{array}{l} -G_{11}q_1 - G_{12}q_2 + H_{13}u_3 + \cdots + H_{1n}u_n = -H_{11}\hat{u}_1 - H_{12}\hat{u}_2 + G_{13}\hat{q}_3 + \cdots + G_{1n}\hat{q}_n \\ -G_{21}q_1 - G_{22}q_2 + H_{23}u_3 + \cdots + H_{2n}u_n = -H_{21}\hat{u}_1 - H_{22}\hat{u}_2 + G_{23}\hat{q}_3 + \cdots + G_{2n}\hat{q}_n \\ \vdots \\ -G_{n1}q_1 - G_{n2}q_2 + H_{n3}u_3 + \cdots + H_{nn}u_n = -H_{n1}\hat{u}_1 - H_{n2}\hat{u}_2 + G_{n3}\hat{q}_3 + \cdots + G_{nn}\hat{q}_n, \end{array}$$

which is the expanded form of Eq (2.8).

As mentioned above, `Sys1` uses the two functions: `Quad1` and `Diag1`. The function `Quad1` computes the off-diagonal elements of H and G by using the Gauss-Legendre quadrature formula. The variable `Ra` is explained in Fig. 2.5(a). In order to compute H_{ij} and G_{ij}, $i \neq j$, we consider two different nodes i and j in Fig. 2.5(a), where (x_p, y_p) are the coordinates of the node i under consideration; ζ_k, $k = 1, 2, 3, 4$ are the Gauss points (nodes) marked on the element with mid-node j; $\zeta = 1$ and $\zeta = -1$ are the extreme points with coordinates (x_j, y_j) and (x_{j+1}, y_{j+1}) respectively of the node j; m denotes the slope of the boundary element with node j; and `Ra` is the distance from node i to a Gauss point (nodes) ζ_k, $k = 1, 2, 3, 4$ (Fig. 2.5(a)). The coordinates of the Gauss points (nodes) are denoted by (Xg, Yg). If we denote `Ax` $= (x_{j+1} - x_j)/2$, `Ay`$= (y_{j+1} - y_j)/2$, `Bx`$= (x_{j+1} + x_j)/2$, and `By` $= (y_{j+1} + y_j)/2$, then $m = (y_{j+1} - y_j)/(x_{j+1} - x_j)$ =`Ay/Ax`=`slope` of the element $\tilde{C}_j$. Also, the equation of the element with node j is

$$m(x_j - x) - (y_j - y) = 0,$$

the distance

$$\texttt{Ra} = \sqrt{(x_p - Xg)^2 + (y_p - Yg)^2},$$

and the half-length of the element $\tilde{C}_i$

$$\frac{L_i}{2} = \sqrt{\texttt{Ax}^2 + \texttt{Ay}^2} = \texttt{HL}.$$

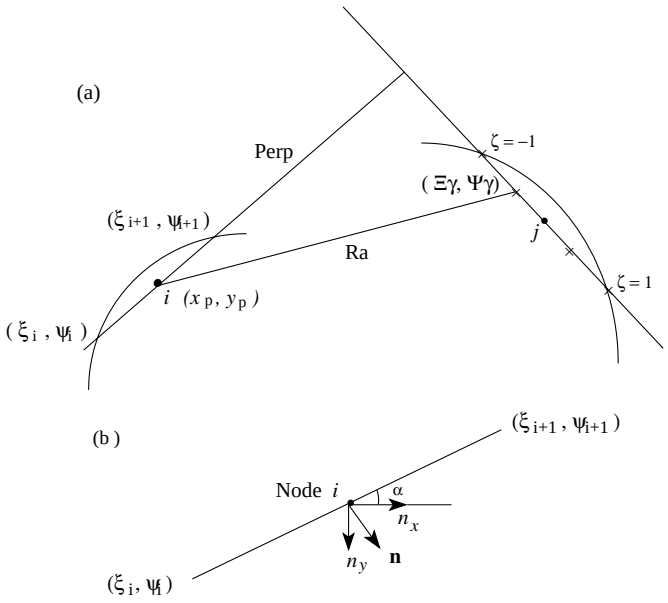

Fig. 2.5.

Also, the directional derivative of $\ln(1/r) = -\frac{1}{2}\ln(x^2+y^2)$ in the direction of $\hat{\mathbf{n}}$ is given by

$$D_{\hat{\mathbf{n}}}\ln(\frac{1}{r}) = \nabla f \cdot \hat{\mathbf{n}} = -\frac{y}{x^2+y^2}$$
$$= -\frac{r_{,x}n_x + r_{,y}n_y}{r^2} = -\frac{\mathtt{rx}\cdot\mathtt{nx} + \mathtt{ry}\cdot\mathtt{ny}}{(\mathtt{Ra})^2},$$

where $\mathtt{rx} = (\mathtt{Xg} - x_p)/\mathtt{Ra} = \cos\alpha$, $\mathtt{ry} = (\mathtt{Yg} - x_p)/\mathtt{Ra} = \sin\alpha$ (see Fig. 2.5(a),(b)). Then, by an 4-point Gauss-Legendre quadrature, we have

$$G_{ij} = \int_{\tilde{C}_j} u^*\, ds = \sum_{i=1}^{4} \ln\left(\frac{1}{\mathtt{Ra}}\right) W_i \sqrt{\mathtt{Ax}^2 + \mathtt{Ay}^2}, \tag{2.14}$$

$$H_{ij} = \int_{\tilde{C}_j} q^*\, ds = \sum_{i=1}^{4} D_{\hat{\mathbf{n}}}\ln(\frac{1}{r})_i W_i \frac{\sqrt{(x_j - x_{j+1})^2 + (y_j - y_{j+1})^2}}{2}$$
$$= -\sum_{i=1}^{4} \frac{1}{(\mathtt{Ra})_i^2} \left(\mathtt{rx}\cdot\mathtt{nx} + \mathtt{ry}\cdot\mathtt{ny}\right) W_i \sqrt{\mathtt{Ax}^2 + \mathtt{Ay}^2}. \tag{2.15}$$

We can use a Gauss-Legendre quadrature formula with different Gauss points (nodes). An empirical rule to decide which one of the Gauss-Legendre quadrature formulas can be used is as follows: Let

$$s = \frac{1}{2L_j}\sqrt{\big(2x_p - X(1) - X(2)\big)^2 + \big(2y_p - Y(1) - Y(2)\big)^2}, \tag{2.16}$$

where (x_p, y_p) are the coordinates of the node i, and $X(j), Y(j), j = 1, 2$, are the coordinates of the extreme points of the node j of the element of length L_j. Then, use 6-point Gauss-Legendre

quadrature formula if $s \leq 1.5$, 4-point formula if $1.5 < s < 5.5$, and 2-point formula if $s \geq 5.5$. However, the 4-point formula gives good results in the constant and linear cases, whereas a 10-point formula is used with advantage in the quadratic and higher order boundary elements.

`Diag1` computes the diagonal elements G_{ii} of the matrix G given by (2.12).

`Solve` uses the Gauss elimination method to solve the system of equations $AX = F$ by providing interchange of rows when a zero diagonal element is present.

Note that since the fundamental solution in the program is taken as $\ln(1/r)$, and not $\frac{1}{2\pi}\ln(1/r)$, all elements of H and G are divided by 2π in the end before the output is produced.

`Inter1` computes the values of u at interior points by using (2.9). It reorders `Bc` (boundary condition vector) and `F` (unknown vector) such that all values of u are stored in `Bc` and all values of q in `F`. Note that since all H and G terms appear multiplied by 2π, the solution for interior points is also finally divided by 2π.

We present some examples. *Read §9 (last section) before running this and other programs.*

EXAMPLE 2.1. Heat flow problem in the region shown in Fig. 2.6 is the simplest case of a linear one-directional flow.

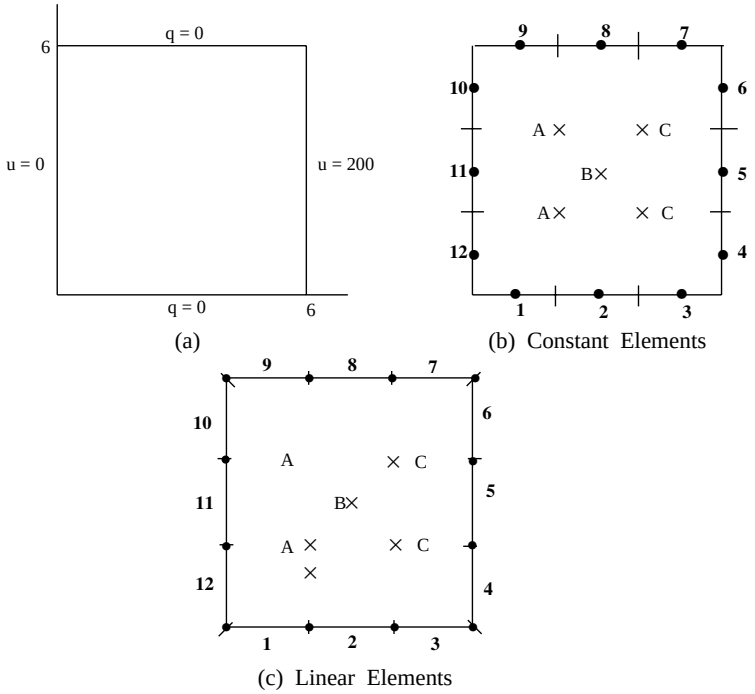

Fig. 2.6.

The input file is `ex2.1.in` and the output file is `ex2.1.out`. The exact solution for the problem $\nabla^2 u = 0$ with $u(0, y) = 0, u(a, y) = T_0$ is given by $u(x, y) = \frac{T_0}{a}x$. In this example, $a = 6$, $T_0 = 200$ gives the exact $u = 100x/3$, and $q_x = 100/3$, $q_y = 0$. ∎

EXAMPLE 2.2. Consider the potential/heat transfer problem represented in Fig. 2.7. The input file is `ex2.2.in` and the output file is `ex2.2.out`. ■

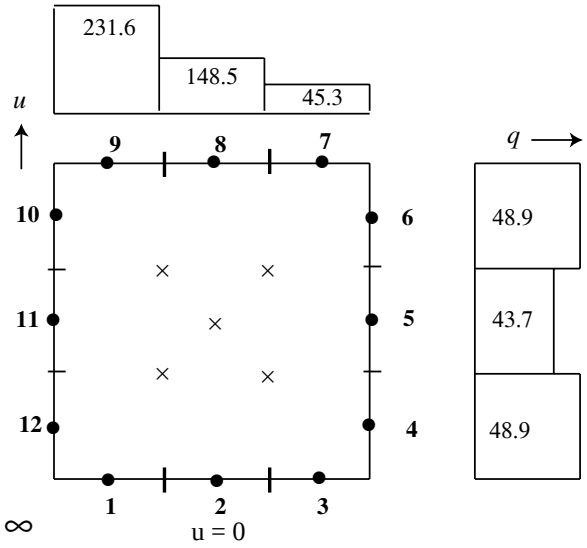

Fig. 2.7.

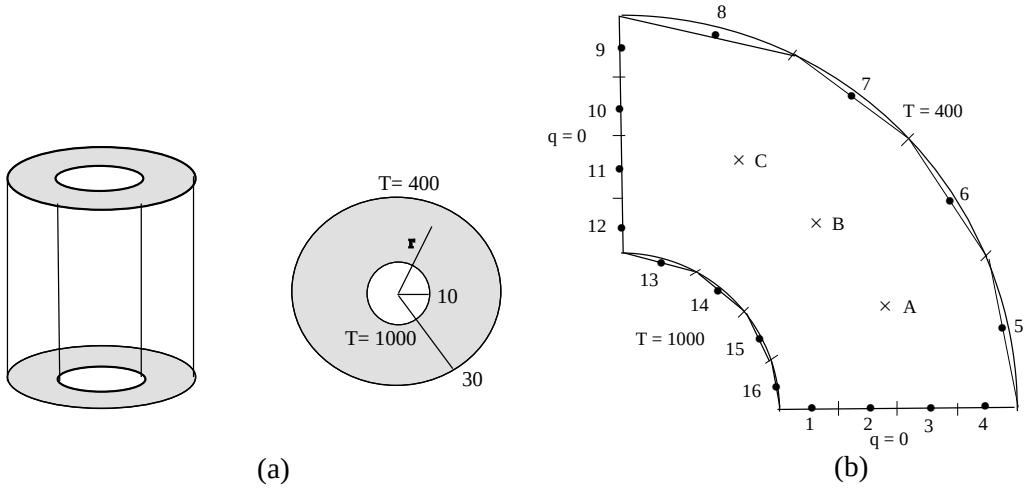

Fig. 2.8.

EXAMPLE 2.3. Consider the heat transfer in a hollow circular cylinder of radii 10 and 30 (Fig. 2.8(a)). Because of the axial symmetry we discretize the quarter region into 16 constant elements (Fig. 2.8(b)). The input file is `ex2.3.in` and the output file is `ex2.3.out`. Exact solution for a hollow cylinder of inner and outer radius a and b respectively is given by

$$T = T_a + \frac{T_a - T_b}{\ln(a/b)} \ln \frac{r}{a}, \quad 10 \le r \le 30,$$

where T_a and T_b are the prescribed temperatures on the circular boundaries $r = a$ and $r = b$ respectively. Exact $T(20) = 621.1442$. A better accuracy is achieved by taking more elements on the circular boundaries. See also Example 2.8. ∎

2.2. Linear Elements. The variation of u and q is assumed to be linear within each element. The nodes are at the intersection of straight elements, and hence called extreme nodes (Fig. 2.2(b)). In this case the BI Eq (1.14) leads to the BE Eq

$$c(i)u(i) + \sum_{j=1}^{N} \int_{\tilde{C}_j} uq^* \, ds = \sum_{j=1}^{N} \int_{\tilde{C}_j} qu^* \, ds \tag{2.17}$$

for N elements. Unlike Eq (1.14), we cannot take u_j and q_j out of the integral sign since they vary linearly within each element. Also, $c(i) = 1/2$ only for smooth boundaries. For nonsmooth boundaries, we will discuss a method to determine $c(i)$ later (see §2.3).

The (Lagrange) interpolation functions for a linear element in normal coordinate system are

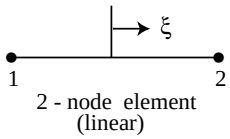

2 - node element
(linear)

$$\phi_1 = \frac{1}{2}(1-\xi) \qquad \phi_2 = \frac{1}{2}(1+\xi). \tag{a}$$

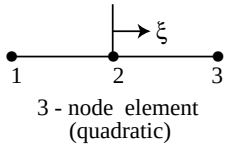

3 - node element
(quadratic)

$$\phi_1 = -\frac{1}{2}\xi(1-\xi) \qquad \phi_2 = (1-\xi^2) \qquad \phi_3 = \frac{1}{2}\xi(1+\xi). \tag{b}$$

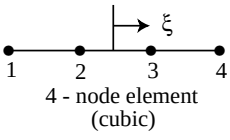

4 - node element
(cubic)

$$\phi_1 = -\frac{9}{16}(1-\xi)(1/9-\xi^2) \qquad \phi_2 = \frac{27}{16}(1-\xi^2)(1/3-\xi)$$
$$\phi_3 = \frac{27}{16}(1-\xi^2)(1/3+\xi) \qquad \phi_4 = -\frac{9}{16}(1+\xi)(1/9-\xi^2). \tag{c}$$

Fig. 2.9. Linear Elements in the Normal Coordinate System.

Note that the interpolation functions $\phi_i(\xi_j)$ are chosen such that

$$\phi_i(\xi_j) = \delta_{ij} = \begin{cases} 1, & \text{if } i = j \\ 0, & \text{if } i \neq j, \end{cases}$$

where ξ_j denotes the ξ-coordinate of the j-th node of the element, ϕ_i $(i = 1, \ldots, n)$ are polynomials of degree $n-1$ (n being the number of nodes in the element), and δ_{ij} is the Kronecker delta.

Consider an arbitrary segment as shown in Fig. 2.9(a). The values of u and q at any point of this segment can be determined in terms of their nodal values and two linear interpolation functions ϕ_1

and ϕ_2 such that, for the case of both u and q varying linearly, we have

$$\begin{aligned} u(\xi) &= \phi_1 u_1 + \phi_2 u_2 = [\phi_1\, \phi_2]\,[u_1\, u_2]^T, \\ q(\xi) &= \phi_1 q_1 + \phi_2 q_2 = [\phi_1\, \phi_2]\,[q_1\, q_2]^T, \end{aligned} \tag{2.18}$$

where ξ is the dimensionless coordinate $\xi = x/(l/2) = 2x/l$, and $\phi_1 = \frac{1}{2}(1-\xi)$, $\phi_2 = \frac{1}{2}(1+\xi)$. The integrals along the element j on the left side of Eq (2.17) is

$$\begin{aligned} \int_{\tilde{C}_j} uq^*\, ds &= \int_{\tilde{C}_j} [\phi_1\ \phi_2]\ [u_1\ u_2]^T q^*\, ds = \int_{\tilde{C}_j} [\phi_1\ \phi_2] q^*\, ds\, [u_1\ u_2]^T \\ &= [h_{i1}\ h_{i2}]\,[u_1\ u_2]^T, \end{aligned} \tag{2.19}$$

where

$$h_{i1} = \int_{\tilde{C}_j} \phi_1 q^*\, ds \equiv a_1, \quad h_{i2} = \int_{\tilde{C}_j} \phi_2 q^*\, ds \equiv a_2. \tag{2.20}$$

For the right side of Eq (2.17)

$$\int_{\tilde{C}_j} qu^*\, ds = \int_{\tilde{C}_j} [\phi_1\ \phi_2] u^*\, ds\, [q_1\ q_2]^T = [g_{i1}\ g_{i2}]\,[q_1\ q_2]^T, \tag{2.21}$$

where

$$g_{i1} = \int_{\tilde{C}_j} \phi_1 u^*\, ds \equiv b_1, \quad g_{i2} = \int_{\tilde{C}_j} \phi_2 u^*\, ds \equiv b_2. \tag{2.22}$$

Substituting (2.19) and (2.21) for all j elements into (2.17), we get for node i

$$c(i)u(i) + \left[\hat{H}_{i1}\ \hat{H}_{i2}\ \cdots\ \hat{H}_{in}\right]\left[u_1\ u_2\ \cdots\ u_n\right]^T = \left[G_{i1}\ G_{i2}\ \cdots\ G_{in}\right]\left[q_1\ q_2\ \cdots\ q_n\right]^T, \tag{2.23}$$

where

$$\hat{H}_{ij} = h_{i1} \text{ term of element } j + h_{i2} \text{ term of element } (j-1) = a_1 + a_2. \tag{2.24}$$

Similarly

$$G_{ij} = g_{i1} \text{ term of element } j + g_{i2} \text{ term of element } (j-1) = b_1 + b_2. \tag{2.25}$$

Formulas (2.23) and (2.25) represent the assembled equation for the collocation point i. For $i = j$,

$$G_{ii} = \frac{1}{2\pi}\int_{\tilde{C}_i} u^*\, ds = \frac{1}{2\pi}\int_{\tilde{C}_i} \left[u_1\phi_1 + u_2\phi_2\right] ds = \frac{1}{2\pi}\left(u_1 G^1_{ii} + u_2 G^2_{ii}\right). \tag{2.26}$$

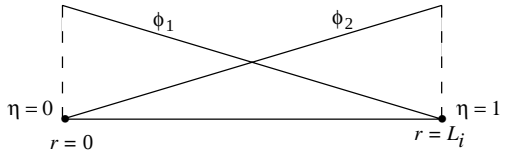

Fig. 2.10.

But in this case we find that although the interpolation functions $\phi_{1,2} = \frac{1}{2}(1 \mp \xi)$ are used in the evaluation of H_{ii}, they fail to remove the singularity at $\xi = 0$ when used to compute G_{ii}. Therefore,

we modify the function $\phi_{1,2}$ by using the translation $\xi = 1 - 2(1-\eta)$, which yields $\phi_1 = 1-\eta$ and $\phi_2 = \eta$, $0 \le \eta \le 1$. Then, using the substitution $r = L_i\eta$, so that $ds = dr = L_i d\eta$ (see Fig. 2.10), we get

$$\begin{aligned} G^1_{ii} &= \int_{\tilde{C}_i} \phi_1 \ln\left(\frac{1}{r}\right)\, ds = \int_0^1 (1-\eta)\ln\left(\frac{1}{L_i\eta}\right) L_i\, d\eta \\ &= L_i \int_0^1 (1-\eta)\,(-\ln L_i - \ln\eta)\; d\eta = \frac{L_i}{2}\left[\frac{3}{2} - \ln L_i\right], \end{aligned} \tag{2.27}$$

$$\begin{aligned} G^2_{ii} &= \int_{\tilde{C}_i} \phi_2 \ln\left(\frac{1}{r}\right)\, ds = \int_0^1 \eta\ln\left(\frac{1}{L_i\eta}\right) L_i\, d\eta \\ &= L_i \int_0^1 \eta\,(-\ln L_i - \ln\eta)\; d\eta = \frac{L_i}{2}\left[\frac{1}{2} - \ln L_i\right]. \end{aligned} \tag{2.28}$$

We can now write Eq (2.23) as

$$c(i)u(i) + \sum_{j=1}^{n} \hat{H}_{ij}u_j = \sum_{j=1}^{n} G_{ij}q_j, \tag{2.29a}$$

or

$$\sum_{j=1}^{n} H_{ij}u_j = \sum_{j=1}^{n} G_{ij}q_j, \tag{2.29b}$$

or, in matrix form, as

$$HU = GQ. \tag{2.29c}$$

Note that the value $-u/2$ obtained in (1.11) is now not valid unless the curve/surface is smooth. We can always compute the diagonal terms of H by using the fact that when a uniform potential is applied over the entire boundary, the normal derivative (i.e., q values) must be zero. Hence, Eq (2.29c) becomes $HU = 0$. However, the sum of all elements of H in any row cannot be zero, and the value of the diagonal elements can be easily evaluated once all off-diagonal elements are known, by using

$$H_{ii} = 1 - \sum_{j=1, j\ne i}^{N} H_{ij}. \tag{2.30}$$

Therefore, we need not compute the value of $c(i)$ explicitly. Also, since the fundamental solution in the program is taken as $-\ln r$, and not as $-\ln r/(2\pi)$, Eq (2.30) is written in the program as

$$H_{ii} = 2\pi - \sum_{j=1, j\ne i}^{N} H_{ij}, \quad i = 1, \ldots, N. \tag{2.31}$$

The results are then finally divided by 2π before the output is produced. The solution at the interior points is also finally divided by 2π in `Inter2` (see program Be2 in the next section). This technique, simple as it is, is maintained throughout all computer programs to ensure uniformity.

2.3. Discontinuous Elements. A corner node becomes significant in linear and higher elements where the second node (marked i) of the $(i-1)$-st element is the same as the first node

of the i-th element $\tilde{C}_i$ (Fig. 2.11(a)). If the potential is the same throughout the boundary, then the value of u on the $\tilde{C}_{i-1}$ is the same as on $\tilde{C}_i$. But this is not, in general, true for the flux q at a corner since the normals to the adjacent elements may be different, and hence not unique, at a corner; or the prescribed value of q along an element may possess discontinuities at some points. The former situation which occurs in most physical problems is solved by rearranging the terms in (2.23)–(2.25), which leads to the BE Eq

$$c(i)u(i) + \sum_{j=1}^{N} \hat{H}_{ij} u_j = \sum_{j=1}^{2N} G_{ij} q_j, \tag{2.32}$$

where the upper limit $2N$ of right sum corresponds to the case when the value of q at node i for the element $\tilde{C}_i$ is different from that for the element $\tilde{C}_{i-1}$ (see Fig. 2.11(b)). Defining, as in (2.4),

$$H_{ij} = \begin{cases} \hat{H}_{ij} & \text{for } i \neq j \\ \hat{H}_{ij} + c(i) & \text{for } i = j, \end{cases} \tag{2.33}$$

we get the same matrix form of the BE Eq as in (2.5), where G is now a $N \times 2N$ matrix.

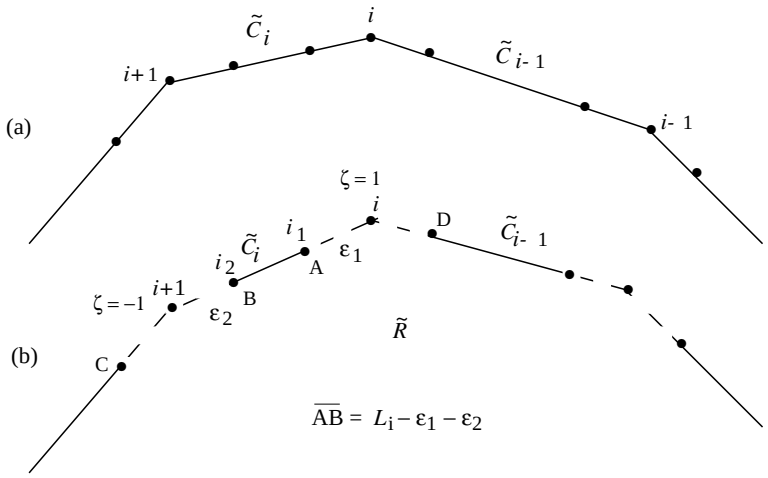

Fig. 2.11.

The following observations are worth noting: At a corner node the flux 'before' and 'after' the node (i.e., the prenodal and postnodal fluxes) may be the same, or they may be prescribed differently. A similar situation may occur for the prescribed potential. However, only one of these variables will be unknown at a node. The following four cases arise at a corner node depending on adjacent boundary conditions:

(i) The prenodal and postnodal values of q are known (unknown: values of u);

(ii) The value of u and the prenodal value of q are known (unknown: postnodal value of q);

(iii) The value of u and the postnodal value of q are known (unknown: prenodal value of q); and

(iv) The values of u are known (unknown: both pre- and postnodal values of q).

Except for the case (iv), there is only one unknown in the three cases which can be computed by using (2.32) and solving the subsequent matrix equation $HU = GQ$. The case (iv) can be

computed by making the two adjacent elements at a corner into two discontinuous elements, by replacing the corner node i into two nodes i_1 and i_2 arbitrarily close to i such that $|i - i_1| = \varepsilon_1$ and $|(i+1) - i_2| = \varepsilon_2$, and $\xi_{i_1} = 2\varepsilon_1/L_i - 1$, and $\xi_{i_2} = 1 - 2\varepsilon_2/L_i$ are the local coordinates of the nodes i_1 and i_2, and the values of u and q prescribed at node i are now assigned to the nodes i_1 and i_2 (Fig. 2.11(b)). Since Eqs (2.18) hold, we have

$$\left\{ \begin{array}{c} u_{i_1} \\ u_{i_2} \end{array} \right\} = \left[\begin{array}{cc} \phi_1(\xi_{i_1}) & \phi_2(\xi_{i_1}) \\ \phi_1(\xi_{i_2}) & \phi_2(\xi_{i_2}) \end{array} \right] \left\{ \begin{array}{c} u_1 \\ u_2 \end{array} \right\}. \tag{2.34}$$

Substituting (2.34) into (2.18) we find that

$$u(\xi) = [\phi_1 \quad \phi_2]\, \mathbf{Q}\, [u_{i_1} \quad u_{i_2}]^T, \tag{2.35}$$

$$q(\xi) = [\phi_1 \quad \phi_2]\, \mathbf{Q}\, [q_{i_1} \quad q_{i_2}]^T, \tag{2.36}$$

where

$$\mathbf{Q} = \frac{1}{L_i - \varepsilon_1 - \varepsilon_2} \left[\begin{array}{cc} L_i - \varepsilon_2 & -\varepsilon_1 \\ -\varepsilon_2 & L_i - \varepsilon_1 \end{array} \right], \tag{2.37}$$

where $L_i - \varepsilon_1 - \varepsilon_2$, denoted by $\overline{AB}$ in Fig. 2.11(b), is the length of the discontinuous element $\tilde{C}_i$. It should be noted that the coefficient $c(i) = 1/2$ for discontinuous elements. The integrals $h_{i_1 1}$, $h_{i_2 1}$, $g_{i_1 1}$, $g_{i_2 1}$ along the discontinuous elements are then given by

$$h_{i_k 1} = \int_{\tilde{C}_j} \phi_k \mathbf{Q} q^*\, ds, \quad g_{i_k 1} = \int_{\tilde{C}_j} \phi_k \mathbf{Q} u^*\, ds, \; k = 1, 2, \tag{2.38}$$

which are evaluated by Gauss-Legendre quadrature for the case when the node i does not belong to the element. In the case when the node i belongs to the element, $h_{i_1 j} = 0 = h_{i_2 j}$, and $g_{i_1 j}$, $g_{i_2 j}$ are obtained by integration as in (2.26). For the corner nodes, as shown in Fig. 2.11(b), the segments AD, BC must be treated like additional linear elements. The linear elements of the type AD, BC may be further discretized to smoothen the corners out, which are thus replaced by polygonal curves.

Besides corner nodes, discontinuous elements also arise in certain cases where the potential u is undefined (and hence discontinuous) at a point on the boundary C. Example 2.7 discusses this type of discontinuous elements. For linear elements we will use the program Be2 which is described below.

Program Be2

This program carries out the computer implementation of the case of linear and discontinuous elements. It deals with the case of Figs. 2.2.(b) and 2.11, and solves the orthotropic potential boundary value problems where u and q vary linearly along the boundary elements, with the nodes same as the extreme points. The Input file is created as, e.g., Be2.in, and it follows the same format as in Be1.in. However, it should be noted that in this case the dimension of the array `Bc` becomes $2N$, since there are two boundary conditions for each element (one at each node). The dimension of the array `F` remains N. The Output file is created as Be2.out which can be typed (on the monitor screen), printed (as hard copy), or used as input for a graphics subroutine. The program calls the following functions: `Sys2, Quad2, Diag2, Inter2`, and `Solve`.

`Quad2` differs from `Quad1` in that instead of computing only one value for the boundary element $\tilde{C}_i$ along which the integration is carried out, it computes the elements of the matrices H and G corresponding to the adjacent nodes i and $(i \pm 1)$.

`Diag2` is a little different from `Diag1`; it computes the elements of the matrix G along the boundary elements which include the node under consideration.

`Inter2` computes the potential at interior points as given by (2.9), but the values of G_{ij} and $\hat{H}_{ij}$ to be used in (2.9) are defined by (2.23)–(2.28).

Dictionary of Variables. In addition to the variable defined in the program Be1, the following variables are also used:

`ux, uy` $u_{,x}, u_{,y}$ defined analogous to (2.11).
`qx, qy` $q_{,x}, q_{,y}$ defined analogous to (2.11).

EXAMPLE 2.4. We solve Example 2.1 with linear elements; use Fig. 2.6(c). The input file is `ex2.4.in` and the output file is `ex2.4.out`. ∎

EXAMPLE 2.5. Solve the Laplace equation $\nabla^2 u = 0$ for an elliptic region R, shown in Fig. 2.12, with the semi-axes 2 and 1 respectively, and the boundary condition $u = (x^2 + y^2)/2$ on C. Because of the symmetry about both x and y axes, we consider the quarter region with 11 linear elements (11 nodes). The input file is `ex2.5.in` and the output file is `ex2.5.out`. Note that the first 10 extreme points, marked 1 through 10 in Fig. 2.12, are given by $x_j = 2\cos j\pi/18$, $y_j = \sin j\pi/18, j = 0, 1, \ldots, 9$. ∎

EXAMPLE 2.6. This is an example of discontinuous elements at corner nodes. The input file from Fig. 2.13 is `ex2.6.in` and the ouput file is `ex2.6.out`. ∎

EXAMPLE 2.7. Solve the Laplace equation $\nabla^2 u = 0$ in the upper-half circular region of radius 10 (Fig. 2.14(a)). The problem has a discontinuous potential at $x = 0$ where the flux has a singularity. We treat the first and the last element as discontinuous elements, although the point $x = 0$ does not qualify as a corner (Fig. 2.14(b)). The input file from Fig. 2.13 is `ex2.7.in` and the ouput file is `ex2.7.out`.

The exact solution is

$$u(x, y) = \frac{100}{\pi}\left(\pi - \arctan\frac{y}{x}\right), \quad 0 < |x| \le 10, 0 \le y \le 10.$$

The flux along the x-axis is given by $q = -100/\pi x$, $0 < |x| \le 10$, whereas on the circumference by

$$q = \frac{100}{(x^2 + y^2)^2}(n_1 y - n_2 x) = 0.$$

The graphs for u, and q along the x-axis are shown in Fig. 2.14(c) and (d), respectively. ∎

EXAMPLE 2.8. We solve the problem of Example 2.3 by treating the four corner nodes as in Fig. 2.15. The input file is `ex2.8.in` and the ouput file is `ex2.8.out`. These results can be compared with Example 2.3. ∎

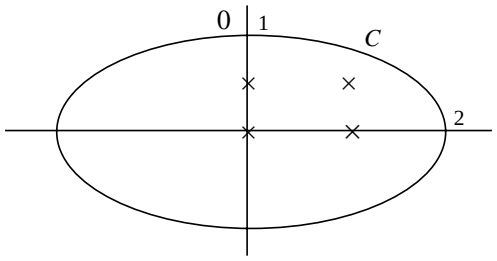

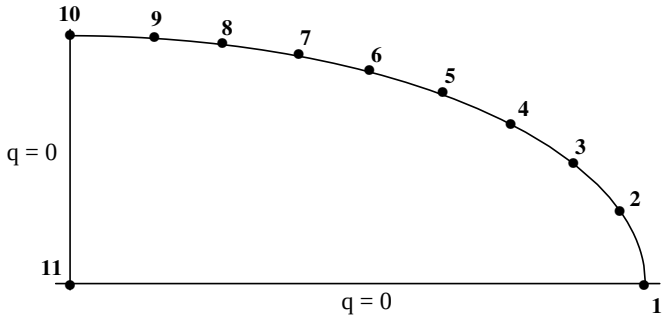

Fig. 2.12.

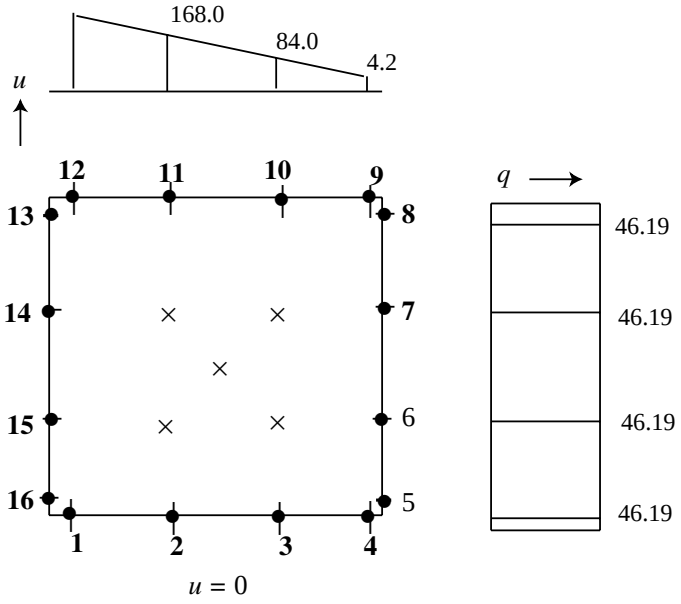

Fig. 2.13.

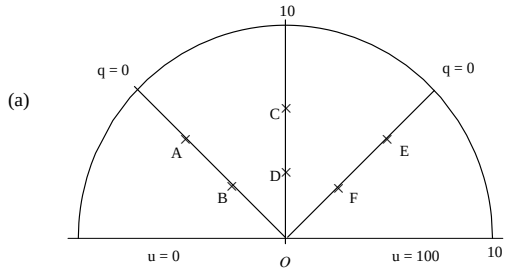

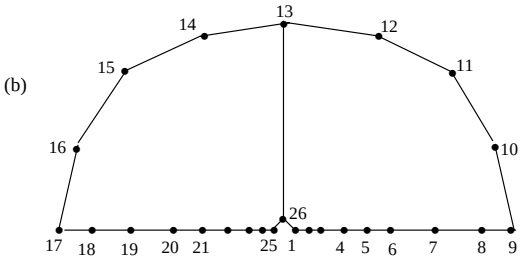

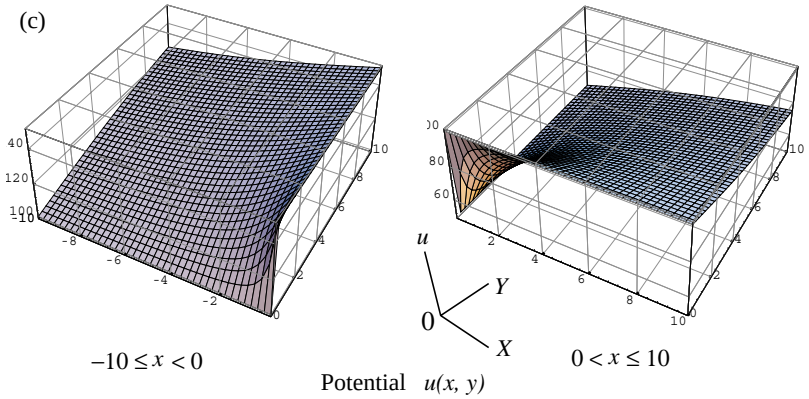

$-10 \le x < 0$ $0 < x \le 10$

Potential $u(x, y)$

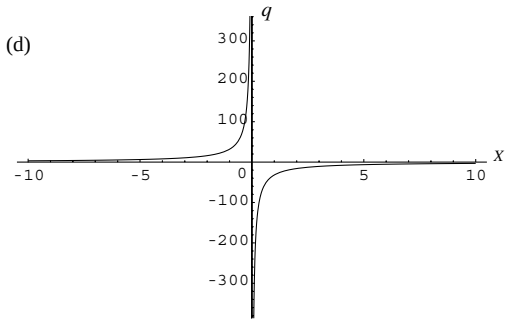

Flux q along x-axis

Fig. 2.14.

2.4. Quadratic and Higher Elements. For quadratic elements (Fig. 2.2(c)) we use the interpolation functions $\phi_1 = -\frac{1}{2}\,\xi(1-\xi)$, $\phi_2 = \left(1-\xi^2\right)$, and $\phi_3 = \frac{1}{2}\,\xi(1+\xi)$. Then the functions u and q are written as

$$\begin{aligned} u(\xi) &= \phi_1 u_1 + \phi_2 u_2 + \phi_3 u_3 = [\phi_1\,\phi_2\,\phi_3][u_1\,u_2\,u_3]^T, \\ q(\xi) &= \phi_1 q_1 + \phi_2 u_2 + \phi_3 u_3 = [\phi_1\,\phi_2\,\phi_3][q_1\,q_2\,q_3]^T. \end{aligned} \tag{2.39}$$

The functions ϕ_1, ϕ_2, ϕ_3 which vary quadratically give the nodal values of the functions when specified for the nodes (see Fig. 2.9(b)). Using these interpolation functions, the evaluation of the integrals along the boundary element j gives (compare with (2.19) and (2.21))

$$\int_{\tilde{C}_j} uq^*\,ds = [h_{j1}\,h_{j2}\,h_{j3}][u_1\,u_2\,u_3]^T, \tag{2.40}$$

where

$$h_{jk} = \int_{\tilde{C}_j} \phi_k q^*\,ds, \quad k = 1,2,3. \tag{2.41}$$

which, using the Jacobian

$$|J| = \frac{ds}{d\xi} = \sqrt{\left(\frac{dx}{d\xi}\right)^2 + \left(\frac{dy}{d\xi}\right)^2} \tag{2.42}$$

yields

$$\int_{\tilde{C}_j} uq^*\,ds = \int_{(1)}^{(2)} u(\xi)|J|q^*\,ds. \tag{2.43}$$

Similarly,

$$\int_{\tilde{C}_j} qu^*\,ds = \int_{\tilde{C}_j} [g_{j1}\,g_{j2}\,g_{j3}][q_1\,q_2\,q_3]^T\,ds, \tag{2.44}$$

where

$$g_{jk} = \int_{\tilde{C}_j} \phi_k u^*\,ds. \tag{2.45}$$

Hence, for node i

$$c(i)u(i) = [\hat{H}_{i1}\,\hat{H}_{i2}\,\cdots\,\hat{H}_{in}][u_1\,u_2\,\cdots\,u_n]^T = [G_{i1}\,G_{i2}\,\cdots\,G_{in}][q_1\,q_2\,\cdots\,q_n]^T, \tag{2.46}$$

where

$$\hat{H}_{ij} = h_{i1} \text{ term of element } (j-1) + h_{i2} \text{ term of element } (j+1) + h_{i3} \text{ terms of element } j, \tag{2.47}$$

and

$$G_{ij} = g_{i1} \text{ term of element } (j-1) + g_{i2} \text{ term of element } (j+1) + g_{i3} \text{ terms of element } j, \tag{2.48}$$

(compare with (2.23)).

It is not easy to evaluate G_{ii} for quadratic elements, as we have done in the cases of constant and linear elements. For better accuracy in numerically computing both H_{ij} and G_{ij}, a 10-point Gauss-Legendre quadrature is recommended. The value of the Jacobian $|J|$, defined by (2.42), is

needed for evaluating (2.43) and (2.44) numerically. It can be computed by defining x and y in terms of the quadratic interpolation functions ϕ_1, ϕ_2, ϕ_3, defined above, as

$$x = \phi_1 x^{\text{node } 1} + \phi_2 x^{\text{node } 2} + \phi_3 x^{\text{node } 3},$$
$$y = \phi_1 y^{\text{node } 1} + \phi_1 y^{\text{node } 2} + \phi_1 y^{\text{node } 3},$$

where the superscript refers to the local node number of a quadratic element. Then the derivatives $\partial x/\partial\xi$ and $\partial y/\partial\xi$ can be easily computed.

3. Poisson Equation. We consider the Poisson boundary value problem

$$\nabla^2 u = b, \quad \text{in } R \tag{3.1}$$

$$u = u_0 \quad \text{on } C_1; \quad \frac{\partial u}{\partial n} \equiv q = q_0 \quad \text{on } C_2, \tag{3.2}$$

where $b = b(x, y)$ and, as before, $C = C_1 \cup C_2$ is the boundary of a two-dimensional region R. As in §1, we will start by taking the test function as u^*, where by $u^* = \dfrac{1}{2\pi} \log \dfrac{1}{|\mathbf{x} - \mathbf{x}'|}$, is the fundamental solution of (1.2). This leads to

$$0 = \iint_R \big(\nabla^2 u - b\big) u^* \, dx\, dy = \iint_R \big(u\nabla^2 u^* - bu^*\big)\, dx\, dy + \int_{C_1} u^* q \, ds + \\ + \int_{C_2} u^* q_0 \, ds - \int_{C_1} u_0 q^* \, ds - \int_{C_2} u q^* \, ds. \tag{3.3}$$

Using $\nabla^2 u^* = \delta(i)$, so that $\displaystyle\iint_R u\nabla^2 u^* \, dx\, dy = -u(i)$, as in (1.3), we obtain

$$-\iint_R bu^* \, dx\, dy - u(i) + \int_{C_1} u^* q \, ds + \int_{C_2} u^* q \, ds - \int_{C_1} u_0 q^* \, ds - \int_{C_2} u q^* \, ds = 0,$$

or

$$\iint_R bu^* \, dx\, dy + u(i) + \int_{C_1} u_0 q^* \, ds + \int_{C_2} u q^* \, ds = \int_{C_1} u^* q \, ds + \int_{C_2} u^* q_0 \, ds, \tag{3.4}$$

or, as in the derivation of (1.14), we obtain the two-dimensional BI Eq as

$$c(i)u(i) + \iint_R bu^* \, dx\, dy + \int_C u q^* \, ds = \int_C u^* q \, ds, \tag{3.5}$$

where $c(i)$ is defined by (1.15). Discretization of (3.5) using constant elements, as in the case of Fig. 2.2(a), leads to the BE Eq

$$c(i)u(i) + \iint_{\tilde{R}} bu^* \, dx\, dy + \sum_{j=1}^{N} u_j \int_{\tilde{C}_j} q^* \, ds = \sum_{j=1}^{N} q_j \int_{\tilde{C}_j} u^* \, ds, \tag{3.6a}$$

or

$$c(i)u(i) + B_i + \sum_{j=1}^{N} \hat{H}_{ij} u_j = \sum_{j=1}^{N} G_{ij} q_j, \tag{3.6b}$$

or

$$B_i + \sum_{j=1}^{N} H_{ij} u_j = \sum_{j=1}^{N} G_{ij} q_j, \tag{3.6c}$$

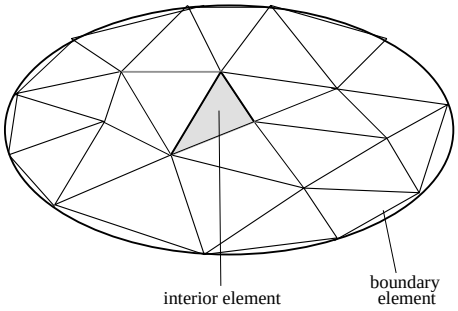

Fig. 3.1. Boundary elements and interior cells.

where H_{ij} is defined by (2.4), and B_i is obtained by integrating the domain integral

$$B_i = \iint_{\tilde{R}} bu^* \, dx \, dy \tag{3.7}$$

numerically as follows: Partition the region $\tilde{R}$ into a mesh of finite elements which are called interior cells (see Fig. 3.1). Note that these interior cells are conceptually different from the usual finite elements although they appear similar. Then use the formula

$$B_i = \sum_{m=1}^{M} \left(\sum_{j=1}^{k} W_j b_j u_j^* \right) A_M, \tag{3.8}$$

where M is the number of interior cells, k the number of integration points on each cell, W_j the weight function, b_j the value of b at integration point j, u_j^* the value of u^* at integration point j,and A_M the area of the cell. Thus, in matrix form, the BE Eq for the N nodes of the type as in Fig. 2.2(a) finally becomes

$$B + HU = GQ. \tag{3.9}$$

Note that N_1 values of u and N_2 values of q are known since they are prescribed on the boundary. We can then reorder (3.9) such that all unknown quantities (called vector X) are on the left side. Then Eq (3.9) becomes

$$AX = F. \tag{3.10}$$

After solving (3.10), we obtain all values of u and q on the boundary nodes. Then we compute the value of u and q at an interior point i by using the formulas (2.9) and (2.10).

EXAMPLE 3.1. Solve the Poisson equation $-\nabla^2 u = 2$ on the elliptic region R shown in Fig. 2.12 with the semi-axes 2 and 1 respectively, and the boundary condition $u = 0$ on C. The solution

of this problem can be divided into two parts: $u = u_1 + u_2$, where $u_1 = -(x^2 + y^2)/2$ is a particular solution and u_2 is the complementary function. Since $-\nabla^2 u_1 = 2$, the problem reduces to the Laplace equation $\nabla^2 u_2 = 0$ with the boundary condition $u_2 = -u_1$ on C, which can be solved as in Example 2.5. A similar problem is discussed in the next example. ∎

EXAMPLE 3.2. The steady Poiseuille flow in a pipe of circular cross section in the direction of z-axis is defined by

$$\mu\left(\frac{\partial^2 u}{\partial x^2} + \frac{\partial^2 u}{\partial y^2}\right) = \frac{\partial p}{\partial z},$$

where u is the fluid velocity in the z-direction, μ its viscosity, and $\partial p/\partial z = -G$ a constant pressure gradient. The flow is then governed by the Poisson equation $-\nabla^2 u = G/\mu$. The exact solution is

$$u(x, y) = \frac{Ga^2b^2}{\mu(a^2 + b^2)}\left(1 - \frac{x^2}{a^2} - \frac{y^2}{b^2}\right).$$

Because of the axial symmetry we will use the quarter region shown in Fig. 2.12. If we take $G/\mu = 2$, we solve $\nabla^2 u_2 = 0$ with the same input file as in Example 2.5. ∎

4. Non-convex Surfaces. The above analysis can be extended to problems on non-convex surfaces (i.e., a region with more than one boundary). An example of such a region is given in Fig. 4.1.

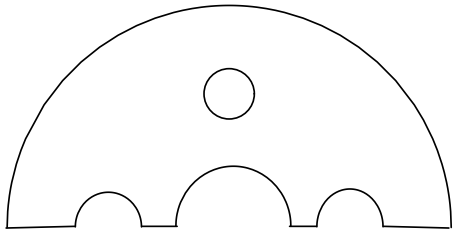

Fig. 4.1. A non-convex surface with one hole

On non-convex surfaces (with holes), the direction of the normal derivatives on the exterior and interior boundaries is determined by the following rule: For exterior boundaries, the numbering scheme for boundary elements is carried out in the counterclockwise direction, whereas for interior boundaries it is defined in clockwise direction. This rule ia analogous to the convention used in contour integration in complex analysis, maintaining the direction on the boundary so that the region always remains to the left. This rule will enable us define the normal derivatives in computer programs.

Program Be5

This program is used for the computer implementation of potential problems on nonconvex surfaces with constant elements (Fig. 2.2(a)). It starts in the same manner as Be1 and adds two new variables:
`M` (≥ 2): Number of different boundaries; if `M` $= 1$, use Be1 or Be2.
`Last`: Number of last node on each different boundary.

Be5 calls the functions `Sys5, Quad1, Diag1, Inter5` and `Solve`.

EXAMPLE 4.1. Solve the Poisson equation on an annular region with boundaries as two concentric circles of radii 1 and 2. We take 8 boundary elements on each circle (see Fig. 4.2, which shows a concentric 8-gon annular region).

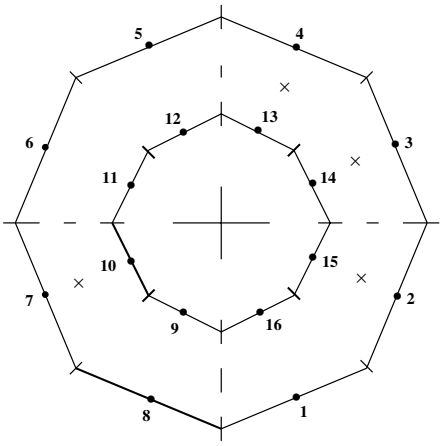

Fig. 4.2.

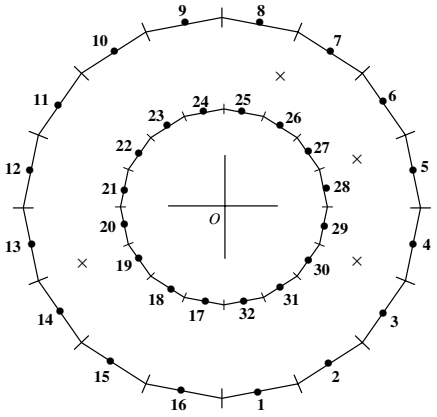

Fig. 4.3.

Thus, there are 16 (constant) boundary elements and 2 different boundaries. The last numbers of the nodes on two surfaces are 8 and 16. As boundary conditions, we assume that $u = 0$ on the exterior boundary and $u = 100$ on the interior boundary. The extreme points are numbered in Fig. 4.2 according to the convention mentioned above. This boundary value problem can be viewed as that of heat transfer between the two concentric circles. Note that

`N`	Number of boundary elements	16
`L`	Number of interior points	4
`M`	Number of different surfaces	2
`Last`	Last node numbers on these surfaces	8, 16

The input file is `ex4.1a.in`, and the output file is `ex4.1a.out`. ∎

For the same problem with 32 boundary elements and `Last` $= 16, 32$ (Fig. 4.3), the input file is `ex4.1b.in`. Note that the coordinates of the outer extreme points are given by

$$x_i = 2\cos\left(\frac{i\pi}{8} - \frac{\pi}{2}\right), \quad y_i = 2\sin\left(\frac{i\pi}{8} - \frac{\pi}{2}\right),$$

and of the inner extreme points by

$$x_i = \cos\left(\frac{i\pi}{8} + \frac{\pi}{2}\right), \quad y_i = -\sin\left(\frac{i\pi}{8} + \frac{\pi}{2}\right), \quad i = 1, \ldots, 16.$$

5. Domain Integral. The presence of the domain integral term B_i, defined by (3.7), in the BE Eq (3.6) introduces numerical integration on interior cells. This means more lengthy computations as compared to those performed for integration on the boundary elements. A method that transform the domain integral into a boundary integral will be helpful in maintaining the computational simplicity of the BEM.

A very simple case is when the function b is constant, linear or harmonic. Then $\nabla^2 b = 0$. Let $v^*(x, y)$ denote a Galerkin-type function such that $\nabla^2 v^* = u^*$. Then, using Green's second identity, we get

$$\iint_R \left(b\nabla^2 v^* - v^*\nabla^2 b\right)\, dx\, dy = \int_C \left(b\frac{\partial v^*}{\partial n} - v^*\frac{\partial b}{\partial n}\right)\, ds, \tag{5.1}$$

which gives

$$B_i = \int_{\tilde{C}} \left(b\frac{\partial v^*}{\partial n} - v^*\frac{\partial b}{\partial n}\right)\, ds, \tag{5.2}$$

Since $u^* = \dfrac{1}{2\pi}\ln\left(\dfrac{1}{r}\right)$, a choice of v^* is obtained by solving $\nabla^2 v^* = u^*$, i.e.,

$$\nabla^2 v^* = \frac{1}{r}\frac{\partial}{\partial r}\left(r\frac{\partial v^*}{\partial r}\right) = \frac{1}{2\pi}\ln\frac{1}{r}, \tag{5.3}$$

which yields

$$v^* = \frac{r^2}{8\pi}\left[1 + \ln\frac{1}{r}\right]. \tag{5.4}$$

If we assume that a source of strength Q_i is concentrated at an interior point i, then

$$b = Q_i\delta(i). \tag{5.5}$$

If finitely many sources are situated at interior points, then the BI Eq (3.5) becomes

$$c(i)u(i) + \int_C uq^*\, ds + B_i + \sum_i Q_i u_i^* = \int_C u^* q\, ds, \tag{5.6}$$

where B_i is now defined by (5.2) as a line integral, and the concentrated sources are easy to compute.

Other methods to transform the domain integral B_i into boundary integrals for different types of the function b will be discussed in detain in Chapter 9.

EXAMPLE 5.1 Consider the Poisson equation $-\nabla^2 u = 2$ in R with the Dirichlet boundary condition $u = 0$ on C, where (a) R is the elliptic region of semi-major axis a_1 and semi-minor axis a_2. In this case the exact solution is given by

$$u = \frac{1}{a_1^{-2} + a_2^{-2}}\left(1 - \frac{x^2}{a_1^2} - \frac{y^2}{a_2^2}\right)$$

(see Example 3.1). Taking $a_1 = 2$ and $a_2 = 1$, we get

Interior point	u (Be2)	u (exact)
$(1.5, 0.0)$	0.345	0.35
$(0.6, 0.45)$	0.563	0.566
$(0.0, 0.45)$	0.634	0.638 ■

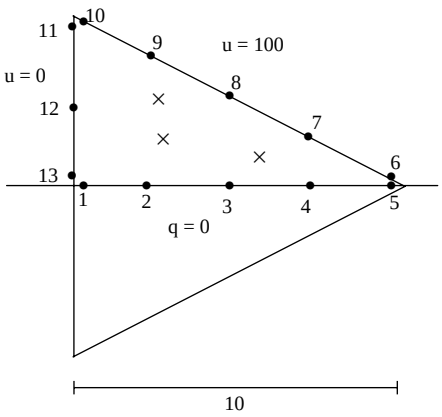

Fig. 5.1.

(b) R is the equilateral triangle of altitude a, (see Fig. 5.1), where, because of the axial symmetry, we have taken 11 linear elements (three discontinuous, one at each corner) in the upper half triangle. The input is `ex5.1b.in`. The exact solution is given by

$$u = \frac{2}{27}a^2 - \frac{1}{2}\left(x^2 + y^2\right) + \frac{1}{2}a\left(x^3 - 3xy^2\right). \blacksquare$$

6. Unbounded Regions. The BI Eq (1.14) is also valid for unbounded regular domains in the following sense: Let R^* be the region exterior to a finite domain D (obstacle) with boundary C, and let K be a circle in R^* of radius r and center at a point i on C (see Fig. 5.2)). Eq (1.14) for the region outside the boundary C and inside the circle K becomes

$$\begin{aligned} c(i)u(i) + \int_C u(x)q^*(\xi,x)\,ds(x) + \int_K u(x)q^*(\xi,x)\,ds(x) \\ = \int_C q(x)u^*(\xi,x)\,ds(x) + \int_K q(x)u^*(\xi,x)\,ds(x). \end{aligned} \tag{6.1}$$

Now let $r \to \infty$ in (6.1). Then the BI Eq for an unbounded region with a cavity should satisfy the condition

$$\lim_{r\to\infty} \int_K [q(x)u^*(\xi,x)\,ds(x) - u(x)q^*(\xi,x)]\,ds(x) = 0. \tag{6.2}$$

The regularity conditions for Eq (6.2) at infinity are as follows: The function u^* behaves like $\ln r$, its derivative q^* is of order $O(1/r)$ as $r \to \infty$, and $ds(x) = |J|\,d\theta = O(r)$, where J is the Jacobian of the transformation from the cartesian to polar cylindrical coordinates. Hence, the two terms in the integral (6.2) do not approach zero separately as $r \to \infty$, but they must cancel each other. Thus, if we apply the condition (6.2) to (6.1) as $r \to \infty$, we obtain the same BE Eq as (1.14), i.e., the BI Eq for an unbounded domain with a cavity is the same as that for finite domains. The same is also true

for points inside an unbounded domain.

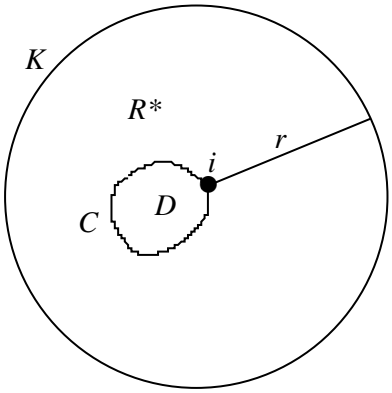

Fig. 6.1. Unbounded region with a finite obstacle

However, in the case of an unbounded domain, the matrix H is not defined like (2.2). Instead, the regularity conditions at infinity will not hold if u is assumed to be constant everywhere in the unbounded domain Ω, where

$$\lim_{r\to\infty}\int_K q^*\,ds = \lim_{r\to\infty}\int_0^{2\pi}\Big(-\frac{1}{2\pi r}\Big)\,r\,d\theta = -1.$$

Hence, the coefficients H_{ii} in the case of an unbounded domain are again given by (2.31).

6.1. Exterior Problems. Consider the exterior problem for the domain shown in Fig. 6.2(a). The boundary of the exterior domain is traversed in the clockwise direction, and the outward normal is directed inward. Suppose we have N boundary elements, which create a closed polygon with N sides and $N+1$ vertices. If we have nodes at each vertex, then there are $N+1$ nodes, numbered from 1 through $N+1$, such that the node 1 and the node $N+1$ coincide. To use formula (1.15) at a corner (vertex), say at node i, the acute angle α_i that lies inside the polygon is actually the exterior angle for this problem. Then the interior angle θ_i for the exterior problem is given by $\theta_i = 2\pi - \alpha_i$. Recall that the angle α_i is the interior angle for the interior problem. To find the angle α_i, we consider three consecutive nodes $i-1$, i, and $i+1$, in the clockwise order, where $i = 1, 2, \ldots, N+1$ (Fig. 6.2(b)).

The cartesian coordinates of all these nodes are known, i.e., the node i has coordinates (x_i, y_i), $i = 1, 2, \ldots, N+1$. Then the angle α_i is found by using the slopes of the sides joining nodes i to $i-1$, and nodes i to $i+1$. Thus,

$$\alpha_i = \Big|\arctan\Big(\frac{y_{i+1}-y_i}{x_{i+1}-x_i}\Big) - \arctan\Big(\frac{y_{i-1}-y_i}{x_{i-1}-x_i}\Big)\Big|.$$

Then the required interior angle for the exterior problem is $\theta_i = 2\pi - \alpha_i$. For the interior angle at node 1 (which is the same as the node $N+1$), use the three consecutive nodes N, 1 and 2 in the above formula to find the angle θ_1 at node 1. Depending on the type of the nodes used, formula (1.15) is used to obtain the value of $c(i)$.

Note that for the exterior problem the program Be1.c (constant elements) is used without any change, i.e., without inserting minus sign in (1.14a), provided the coordinates are used in the clockwise

direction. But in the case of Be2.c, Be5.c and Be11.c, the interior angle θ, which for the exterior problem is $2\pi - \alpha$, needs special attention. These programs are written for the interior problems only. So for the exterior problems the computer code should be modified by replacing the angle θ (of of the interior problem) by $2\pi - \alpha$. recall that the angle α is actually θ for the interior problems. So in the computer codes replace θ by $2\pi - \alpha$, and remember to take the coordinates of all the nodes (corner or otherwise) in the clockwise direction for exterior problems.

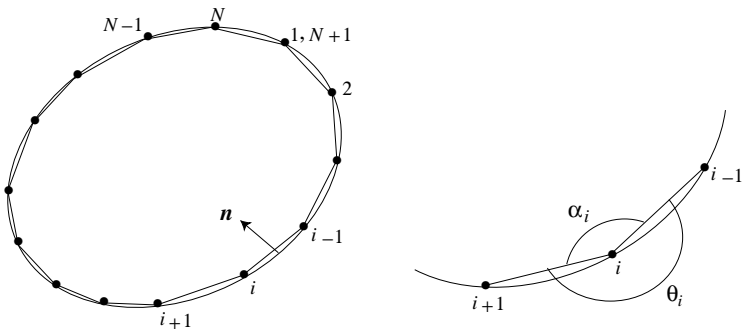

Fig. 6.2.

7. Mixed Boundary Conditions. The mixed boundary conditions play an important role in some boundary value problems. In heat transfer problems, for example, this type of condition has the form $q + \beta(T - T_a) = q_0$, where T is the temperature field, T_a the ambient temperature, β the heat transfer coefficient (also called the film coefficient), and q_0 a prescribed heat flux.

EXAMPLE 7.1. Consider a column of rectangular cross section; a portion of the boundary is subjected to an internal condition, another portion is subjected the exterior weather conditions, and the remaining portion is in contact with the abutting wall which separates both portions (see Fig. 7.1(a)). The prescribed boundary conditions on the internal face ($x = 0$) are: $T_a = 50^o F$ and $\beta = 0.5$ Btu$/(hft^2\ ^oF)$, and on the exterior face ($x = l$): $T_a = 0^o F$ and $\beta = 6.0$ Btu$/(hft^2\ ^oF)$. The temperature and the heat transfer coefficient on the faces $y = \pm 6$ are noted in Fig. 7.1(a). We assume that $q_0 = 0$, and the thermal conductivity is 1.0 Btu$/(hft\ ^oF)$. Because of the symmetry about x-axis, only the half of the structure is discretized into 21 linear elements, and 21 boundary nodes are marked (Fig. 7.1(b)). We assign `Code`$= 2$ for mixed boundary conditions. The input file is created in the following order:

Entry #	Variable	Explanation
1	Title	Must enter problem title.
2	`N`	Number of boundary elements.
3	`L`	Number of interior points where solution is to be computed.
1	`M`	Number of different boundaries
4	`Last`	Number of the last node on each boundary.
next N-pairs	`X, Y`	x, y coordinates of extreme points

next N-triplets `Code`,β, T_a N-triplets of `Code` (2), β and T_a each node, starting with node 1 and ending with node N.

next L-pairs `Xi, Yi` coordinates of interior points where the solution is to be computed.

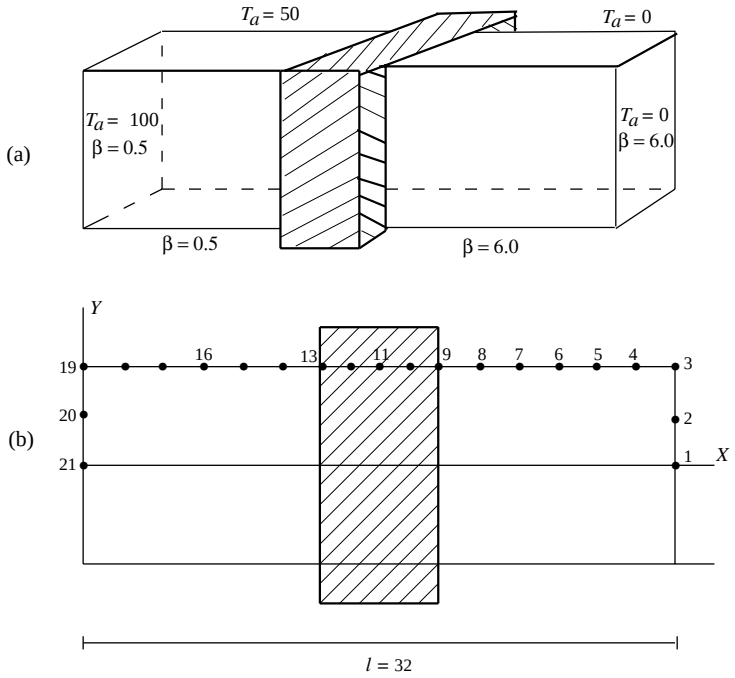

Fig. 7.1. A column with an abutting wall.

The inputfile is `ex7.1.in`. Note that β is assumed to be zero at node 11 as this node is approached from both sides. The value of β is also halved at nodes 12 and 14 respectively from each side. In the above input file, `Code`$= 2$ defines a linear relation between the potential and the flux. An algorithm for generating the boundary conditions for `Code` $= 0, 1$, or 2 can be written as follows: Let F_j denote the value of the potential u if `Code`$= 0$, the value of the flux q if `Code`$= 1$, and the value of the coefficient β if `Code`$= 2$; also, let S_j denote the value of q if `Code`$= 2$; here $j = 1, \ldots, N$, where N is the total number of boundary elements (hence the total number of boundary conditions). Then

$j = 1$
For $i = 1$ to N Do
$i_1 := j$
Read $j, Code_j, F_j, S_j$
$j_1 := j - i_1$
$j_2 := j_1 - 1$
$a_1 :=$ Float(j_1)
$a_x := (F_j - F_{i_1})/a_1;\ a_y := (S_j - S_{i_1})/a_1$

For $n = 1$ to j_2 Do
$i_2 := i_1 + n; i_3 := i_2 - 1$
$Code_{i_2} := Code_{i_3}$
$F_{i_2} := F_{i_3} + a_x;\ S_{i_2} := S_{i_3} + a_y.$

Program Be5 can then be modified accordingly.

Linear Elasticity

8. Linear Elasticity. We will analyze linear elastic continua under the assumption that they undergo small strains. The linear theory of elasticity is based on the following two basic assumptions: (i) The material is subject to an infinitesimal strain and the stress is expressed as a linear function of strain, and (ii) any variation in the orientation of this material due to displacements is negligible. These assumptions lead to small strain and equilibrium equations under an undeformed geometry. The linearity assumption is an attempt to simplify the mathematical aspect of the behavior of solids. Although we assume that the material properties are linear, the deformations in a body may not be completely linear. For example, under certain loads, various materials exhibit plastic deformation while others creep with time, or they may crack in which case the stresses are redistributed.

8.1. Stress and Strain. We will express small strains and related stresses with respect to a right-hand rectangular coordinate system. Thus, in a cartesian system where the coordinates are denoted by $\mathbf{x} = (x_1, x_2, x_3)$, consider an infinitesimal element. The stress vector is defined by

$$\boldsymbol{\sigma} = \begin{bmatrix} \sigma_{11} & \sigma_{12} & \sigma_{13} \\ \sigma_{21} & \sigma_{22} & \sigma_{23} \\ \sigma_{31} & \sigma_{32} & \sigma_{33} \end{bmatrix}. \tag{8.1}$$

Note that if the coordinate system is taken as (x, y, z), instead of (x_1, x_2, x_3), then the normal stresses $\sigma_{11}, \sigma_{22}, \sigma_{33}$ are denoted by $\sigma_x, \sigma_y, \sigma_z$ respectively, and the shearing stresses σ_{12}, σ_{13}, σ_{21}, σ_{23}, σ_{31}, σ_{32} by τ_{xy}, τ_{xz}, τ_{yx}, τ_{yz}, τ_{zx}, τ_{zy} respectively. The equilibrium of the infinitesimal element implies that

$$\sigma_{12} = \sigma_{21}, \quad \sigma_{13} = \sigma_{31}, \quad \sigma_{23} = \sigma_{32}. \tag{8.2}$$

Thus, we need to consider only three independent components of the shearing stress. Corresponding to these stresses, the normal and shearing strains are defined as follows:

$$\begin{aligned} &\text{Normal strains:} \quad \varepsilon_{ii} = u_{i,i}, \quad i = 1, 2, 3, \\ &\text{shearing strains:} \quad \varepsilon_{ij} = \frac{1}{2}\left(u_{i,j} + u_{j,i}\right), \quad i, j = 1, 2, 3 \quad (i \neq j), \end{aligned} \tag{8.3}$$

where (u_1, u_2, u_3) are translations along the (x_1, x_2, x_3) directions respectively. As before, only three of the above shearing strains

The stress tensor σ satisfies the following three equilibrium equations:

$$\frac{\partial \sigma_{ij}}{\partial x_j} + b_i = 0, \quad i, j = 1, 2, 3, \tag{8.4}$$

where b_i are the body forces. The strain-stress relations for an isotropic material are given by

$$\begin{aligned} \varepsilon_{11} &= \frac{\sigma_{11} - \nu\sigma_{22} - \nu\sigma_{33}}{E}, & \varepsilon_{12} &= \frac{\sigma_{12}}{G}, \\ \varepsilon_{22} &= \frac{-\nu\sigma_{11} + \sigma_{22} - \nu\sigma_{33}}{E}, & \varepsilon_{23} &= \frac{\sigma_{23}}{G}, \\ \varepsilon_{33} &= \frac{-\nu\sigma_{11} - \nu\sigma_{22} + \sigma_{33}}{E}, & \varepsilon_{31} &= \frac{\sigma_{31}}{G}, \end{aligned} \tag{8.5}$$

where E is the Young's modulus, G the shear modulus, and ν the Poisson's ratio ($0 < \nu < 1/2$). In matrix form, Eq (8.5) is written as

$$\boldsymbol{\varepsilon} = C\boldsymbol{\sigma}, \tag{8.6}$$

where

$$C = \frac{1}{E}\begin{bmatrix} 1 & -\nu & -\nu & 0 & 0 & 0 \\ -\nu & 1 & -\nu & 0 & 0 & 0 \\ -\nu & -\nu & 1 & 0 & 0 & 0 \\ 0 & 0 & 0 & 2(1+\nu) & 0 & 0 \\ 0 & 0 & 0 & 0 & 2(1+\nu) & 0 \\ 0 & 0 & 0 & 0 & 0 & 2(1+\nu) \end{bmatrix} \tag{8.7}$$

is the matrix that relates the strain vector $\boldsymbol{\varepsilon}$ to the stress vector $\boldsymbol{\sigma}$. The components c_{ij} of the matrix C are called elastic compliances. Inversely, the stress-strain relations from (8.6) are given by

$$\boldsymbol{\sigma} = D\boldsymbol{\varepsilon}, \tag{8.8}$$

where the matrix D which relates the stress vector $\boldsymbol{\sigma}$ to the strain vector ε is

$$\begin{aligned} D = C^{-1} &= \frac{E}{2(1+\nu)(1-2\nu)}\times \\ &\times \begin{bmatrix} 2(1-\nu) & \nu & \nu & 0 & 0 & 0 \\ 2\nu & (1-\nu) & \nu & 0 & 0 & 0 \\ 2\nu & \nu & (1-\nu) & 0 & 0 & 0 \\ 0 & 0 & 0 & 1-2\nu & 0 & 0 \\ 0 & 0 & 0 & 0 & 1-2\nu & 0 \\ 0 & 0 & 0 & 0 & 0 & 1-2\nu \end{bmatrix}. \end{aligned} \tag{8.9}$$

The components d_{ij} of the matrix D are called rigidity coefficients. The relationships (8.6) and (8.8) can also be expressed in terms of the Lame's constants λ, μ which are related to E and $\boldsymbol{\nu}$ by

$$\lambda = \frac{E\varepsilon}{(1+\nu)(1-2\nu)}, \quad \mu = \frac{E}{2(1+\nu)} = G.$$

8.2. Virtual Work. The virtual work δW performed by the external forces $\sigma_{ij,i} + b_j$ and $p_j^0 - p_j$ in a virtual displacement δu_j^* is defined by the equation

$$\begin{aligned} \delta W &= \iiint_V (\sigma_{ij,i} + b_j)\delta u_j^* dV - \iint_{S_2} (p_j - p_j^0)\delta u_j^* dS \\ &= \delta\left[\iiint_V (\sigma ij, i + b_j)u_j^* dV - \iint_{S_2} (p_j - p_j^0)u_j^* dS\right]. \end{aligned}$$

Since $\delta W = 0$ in the equilibrium state, this equation gives the principle of virtual displacements for three dimensional linear elastic problems as

$$\iiint_V (\sigma_{ij,i} + b_j) u_j^* dV - \iint_{S_2} (p_j - p_j^0) u_j^* dS = 0. \tag{8.10}$$

Note that for two dimensional problems, we should replace V by R, dV by $dx\,dy$, S_2 by C_2, and dS by ds in (8.10). Also, note that if u_j^* does not satisfy the homogeneous boundary conditions on S_1 (i.e., if $u_j^* \neq 0$ on S_1), then (8.10) becomes

$$\iiint_V (\sigma_{ij,i} + b_j) u_j^* dV = \iint_{S_1} (u_j^0 - u_j) p_j^* dS + \iint_{S_2} (p_j - p_j^0) u_j^* dS, \tag{8.11}$$

where $p_i^* = \sigma_{ij}^* n_j$ are the tractions relative to the u_i^* system.

The integral relation between the equilibrium stress field and the virtual displacement field is, in general, defined by (8.11) which after applying the divergence theorem yields

$$\iiint_V \left(\sigma_{jk,j} + b_k\right) u_k^* \, dV = \iiint_V \left(b_k u_k^* - \sigma_{jk} \varepsilon_{jk}^*\right) dV + \iint_{S_1+S_2} p_k u_k^* \, dS.$$

Thus,

$$\iiint_V b_k u_k^* \, dV - \iiint_V \sigma_{jk} \varepsilon_{jk}^* \, dV = \iint_{S_1} \left(u_k^0 - u_k\right) p_k^* \, dS - \iint_{S_2} p_k^0 u_k^* \, dS - \iint_{S_1} p_k u_k^* \, dS,$$

where $p_k = n_k \sigma_{jk}$ and $p_k^* = n_k \sigma_{jk}^*$. Since $u_k = u_k^*$ and $\sigma_{jk} = \sigma_{jk}^*$, i.e., $p_k = p_k^*$ on S_1, we find from the above equation that

$$\iiint_V \left(\sigma_{jk,j} + b_k\right) u_k^* \, dV = \iint_{S_1} u_k^0 p_k^* \, dS - \iint_{S_2} p_k^0 u_k^* \, dS - \iint_{S_1} p_k u_k^* \, dS + \iint_{S_2} p_k u_k^* \, dS. \tag{8.12}$$

We know from Eq (8.4) that the fundamental solution for the stress tensor satisfies the (three) equations

$$\sigma_{jk,j}^* + \delta_l(i) = 0, \tag{8.13}$$

where $\delta_l(i)$ is the Dirac delta function which represents a unit load at a point i in a direction l (which can be x_l, $l = 1, 2, 3$). In view of the translation property of the Dirac delta function, we get from (8.13)

$$\iiint_V \sigma_{jk,j}^* u_k \, dV = -\iiint_V \delta_l(i) u_k \, dv = -u_l(i).$$

Thus, we find from (8.12) that the fundamental solution u_k^* will satisfy the integral relation

$$u_l(i) + \iint_{S_1} u_k^0 p_k^* \, dS + \iint_{S_2} p_k u_k^* \, dS = \iiint_V b_k u_k^* \, dV + \iint_{S_1} p_k u_k^* \, dS + \iint_{S_2} p_k^0 u_k^* \, dS,$$

which can be written concisely as

$$u_l(i) + \iint_S u_k p_k^* \, dS = \iiint_V b_k u_k^* \, dV + \iint_S p_k u_k^* \, dS, \tag{8.14}$$

where $S = S_1 + S_2$, $u_k = u_k^0$ on S_1, and $p_k = p_k^0$ on S_2.

Since the displacements u_k^* and the tractions p_k^* $(= n_k \sigma_{lk})$ in the direction l) are the fundamental solutions, these quantities represent the displacements and tractions due to a concentrated unit load at a point i in the direction l. The relation (8.14) is valid for a unit force acting in the three directions X_1, X_2, X_3, where p_{jk}^* denote the surface forces at the point k generated by the unit load at the point i. Thus, if we consider the unit forces acting in the X_1, X_2, X_3 directions, the relation (8.14) can be written as

$$u_l(i) + \iint_S u_k p_{lk}^* \, dS = \iiint_V b_k u_{lk}^* \, dV + \iint_S p_k u_{lk}^* \, dS, \tag{8.15}$$

where u_{lk}^* and p_{lk}^* denote the displacements and tractions applied at the point i and acting in the l direction. Eq (8.15) is known as the Somigliana identity.

In a two-dimensional medium, the fundamental solutions for an isotropic plane strain case are

$$u_{lk}^* = \frac{1}{8\pi\mu(1-\nu)r}\Big[(3-4\nu)\ln\Big(\frac{1}{r}\Big)\delta_{lk} + \frac{\partial r}{\partial x_l}\frac{\partial r}{\partial x_k}\Big], \tag{8.16}$$

$$p_{lk}^* = -\frac{1}{4\pi(1-\nu)}\Big[\frac{\partial r}{\partial n}\Big\{(1-2\nu)\delta_{lk} + 2\frac{\partial r}{\partial x_l}\frac{\partial r}{\partial x_k}\Big\} - -(1-2\nu)\Big(\frac{\partial r}{\partial x_l}n_k - \frac{\partial r}{\partial x_k}n_l\Big)\Big].$$

Note that for the spherical coordinate system, defined by

$$\left.\begin{aligned} x_1 &= r\sin\theta\cos\phi, \\ x_2 &= r\sin\theta\sin\phi, \\ x_3 &= r\cos\theta, \end{aligned}\right\} \qquad \begin{aligned} &0 \le \phi \le 2\pi, \\ &0 \le \theta \le \pi, \end{aligned} \tag{8.17}$$

we have $\dfrac{\partial r}{\partial x_k} = \dfrac{r}{x_k}$, and

$$\frac{\partial r}{\partial x_l}n_k - \frac{\partial r}{\partial x_k}n_l = \frac{\partial r}{\partial x_l}\frac{\partial x_k}{\partial r} - \frac{\partial r}{\partial x_k}\frac{\partial x_l}{\partial r} = 0. \tag{8.18}$$

The fundamental solutions for an isotropic body in a three-dimensional region are given by

$$u_{lk}^* = \frac{1}{16\pi\mu(1-\nu)r}\Big[(3-4\nu)\delta_{lk} + \frac{\partial r}{\partial x_l}\frac{\partial r}{\partial x_k}\Big], \tag{8.19}$$

$$p_{lk}^* = -\frac{1}{8\pi(1-\nu)r^2}\Big[\frac{\partial r}{\partial n}\Big\{(1-2\nu)\delta_{lk} + 3\frac{\partial r}{\partial x_l}\frac{\partial r}{\partial x_k}\Big\} - -(1-2\nu)\Big\{\frac{\partial r}{\partial x_l}n_k - \frac{\partial r}{\partial x_k}n_l\Big\}\Big], \tag{8.20}$$

where r is the distance from the (boundary) point of application of the load (point i in Fig. 8.1) to the (boundary) point under consideration (point k in Fig. 8.1); $\hat{\mathbf{n}}$ is the outward unit normal to the surface S of the body, with n_j as its direction cosines, and δ_{ij} is the Kronecker delta. The

fundamental solutions u^*_{lk} have been derived in §4.4.

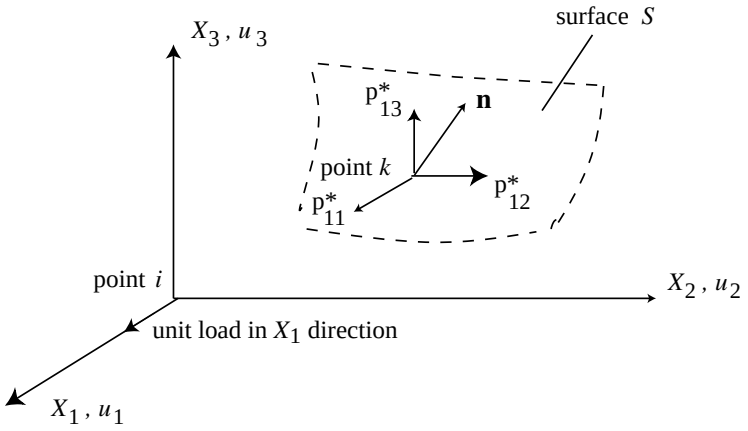

Fig. 8.1. Displacements and Tractions.

8.3. Boundary Integral Equation. We shall start with the integral relation (8.15) and discretize it for the boundary S. Let us assume that the boundary is smooth and it is the part S_2 that contains the point i (the same will hold if the part S_1 contains the point i). If we consider the hemisphere of radius ε on the surface S_2 of a three-dimensional region, as in Fig. 1.1(b), and assume that the point i is at the center of this hemisphere, then in the limiting process the hemisphere reduces to the point i as $\varepsilon \to 0$. This hemisphere divides the surface S_2 into two parts: S_ε and $S_{2-\varepsilon}$. Now, the first integral in Eq (8.15) can be written on S_2 as

$$\iint_{S_2} u_k p^*_{lk}\, dS = \iint_{S_\varepsilon} u_k p^*_{lk}\, dS + \iint_{S_{2-\varepsilon}} u_k p^*_{lk}\, dS.$$

Note that $r = \varepsilon$ and $\partial r/\partial n = 1$ on S_ε. In view of (8.18) and (8.20) we find that

$$\lim_{\varepsilon\to 0} \iint_{S_\varepsilon} u_k p^*_{lk}\, dS = \lim_{\varepsilon\to 0} \Big\{ - \iint_{S_\varepsilon} \frac{u_k}{8\pi(1-\nu)\varepsilon^2} \Big[(1-2\nu)\delta_{lk} + 3\frac{\partial \varepsilon}{\partial x_l}\frac{\partial \varepsilon}{\partial x_k} \Big] \Big\}\, dS.$$

Since $\partial r/\partial x_l = e_l$, we can take, e.g., $l = 1$ in this equation, and then using the spherical coordinate system (8.17), we get

$$\lim_{\varepsilon\to 0} \iint_{S_\varepsilon} u_k p^*_{lk}\, dS = -\frac{1}{8\pi(1-\nu)} \int_0^{2\pi} \int_0^{\pi/2} \big\{ u_1(i)(1-2\nu) + 3u_1(i)\sin^2\theta\cos^2\phi$$
$$+ 3u_2(i)\sin^2\theta\cos\phi\sin\phi + 3u_3(i)\sin\theta\cos\theta\cos\phi \big\} \sin\theta\, d\theta\, d\phi = -\frac{1}{2}u_1(i). \quad (8.21)$$

The same value of the limit of the above integral as $\varepsilon \to 0$ is obtained in the cases when $l = 2$ and 3. Hence, we find that

$$\lim_{\varepsilon\to 0} \iint_{S_\varepsilon} u_k p^*_{lk}\, dS = -\frac{1}{2}\, u_l(i).$$

Now, the last integral in (8.15) on S_2 can be written as

$$\iint_{S_2} p_k u^*_{lk}\, dS = \iint_{S_\varepsilon} p_k u^*_{lk}\, dS + \iint_{S_{2-\varepsilon}} p_k u^*_{lk}\, dS.$$

Since from (8.19)

$$\lim_{\varepsilon\to 0}\iint_{S_\varepsilon} p_k u^*_{lk}\,dS = \lim_{\varepsilon\to 0} p_k u^*_{lk}\cdot 2\pi\varepsilon^2 = 0,$$

and since $S_{2-\varepsilon}\to S_2$ as $\varepsilon\to 0$, and recalling that similar results hold for S_1, we find that Eq (8.15) gives the BI Eq for a smooth boundary surface as

$$\frac{1}{2}u_l(i) + \iint_{S_1} u^0_k p^*_{lk}\,dS + \iint_{S_2} u_k p^*_{lk}\,dS = \iiint_V b_k u^*_{lk}\,dV + \iint_{S_1} p^0_k u^*_{lk}\,dS + \iint_{S_2} p_k u^*_{lk}\,dS. \quad (8.22)$$

In the case of a nonsmooth boundary surface S, the evaluation of the integral of the type (8.21) on S_ε is different from $-\frac{1}{2}u_l(i)$. However, we do not need an exact value in the nonsmooth case. We can take the value of this integral as $c_l(i)u_l(i)$, where $c_l(i)$ is the constant $c(i)$ defined in (1.15) and depends on the geometry of the surface at the point i. Hence, the BI Eq for the nonsmooth body surface can be written, in general, as

$$c_l(i)u_l(i) + \iint_S u_k p^*_{lk}\,dS = \iiint_V b_k u^*_{lk}\,dV + \iint_S p_k u^*_{lk}\,dS. \quad (8.23)$$

The relations (8.22) and (8.23) are the starting point for the boundary element method in linear elastostatics. In the two-dimensional case, the relations (8.22) and (8.23) remain valid if we replace V by R, dV by $dx_1\,dx_2$ (or $dx\,dy$), S by C, and dS by ds.

We will rewrite the BI Eq (8.23) for a two-dimensional isotropic elastic medium. Using the notation $\mathbf{u}^*$ for the displacements u^*_{lk} and $\mathbf{p}^*$ for the tractions p^*_{lk}, we note that both $\mathbf{u}^*$ and $\mathbf{p}^*$ are 2×2 matrices:

$$\mathbf{u}^* = \begin{bmatrix} u^*_{11} & u_{12} \\ u^*_{21} & u^*_{22} \end{bmatrix}, \qquad \mathbf{p}^* = \begin{bmatrix} p^*_{11} & p^*_{12} \\ p^*_{21} & p^*_{22} \end{bmatrix}.$$

These displacements and tractions are in the k direction due to a unit force applied in the l direction. We will further denote the displacement, traction and body forces acting on the body by $\mathbf{u}$, p, b respectively, each of which is defined as a vector, as follows:

$$\mathbf{u} = [u_1\ u_2]^T, \quad \mathbf{p} = [p_1\ p_2]^T, \quad \mathbf{b} = [b_1\ b_2]^T.$$

With this notation, Eq (8.23) becomes

$$\mathbf{c}(i)\mathbf{u}(i) + \int_C \mathbf{p}^*\mathbf{u}\,ds = \iint_R \mathbf{u}^*\mathbf{b}\,dx_1\,dx_2 + \int_C \mathbf{u}^*\mathbf{p}\,ds, \quad (8.24)$$

where R is a plane region (plate) in the X_1X_2-plane (see Fig. 8.2) which depicts the case of constant boundary elements with mid-nodes (cf. with the case of Fig. 2.2(a), and see Fig. 3.1). The interior cells are used for the evaluation of the domain integral $\iint_R \mathbf{u}^*\mathbf{b}\,dx_1\,dx_2$ in (8.24) which contains

the body force terms.

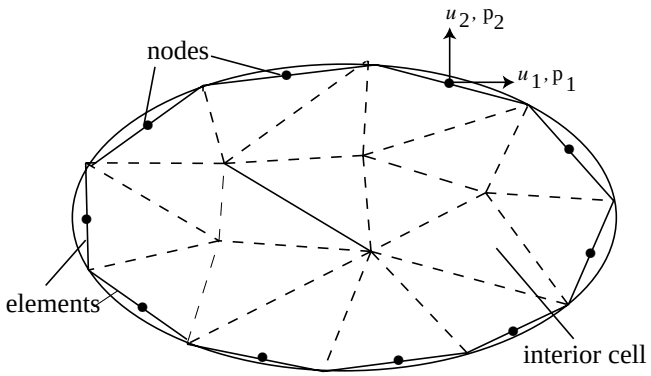

Fig. 8.2. Constant boundary elements and interior cells.

In the case of constant elements, the values of $\mathbf{u}$ and $\mathbf{p}$ are assumed to be constant on each element and equal to their values at its mid-node. Hence, in this case Eq (8.24) reduces to the BE Eq

$$\mathbf{c}(i)\mathbf{u}(i) + \sum_{j=1}^{N}\Big\{\int_{\bar{C}_j} \mathbf{p}^*\, ds\Big\}\,\mathbf{u}_j = \iint_{\bar{R}} \mathbf{u}^*\mathbf{b}\, dx_1\, dx_2 + \sum_{j=1}^{N}\Big\{\int_{\bar{C}_j} \mathbf{u}^*\, ds\Big\}\,\mathbf{p}_j, \tag{8.25}$$

where $\mathbf{u}_j$ and $\mathbf{p}_j$ are the nodal displacement and traction in the element $j = 1, \ldots, N$.

The interior cells are used to numerically integrate the domain integral (body force terms)

$$\mathbf{B}_i = \iint_{\bar{R}} \mathbf{u}^*\mathbf{b}\, dx_1\, dx_2, \tag{8.26}$$

which appears in (8.25) (for interior cells, see §3). If there are M interior cells, then

$$\mathbf{B}_i = \sum_{s=1}^{M}\Big\{\sum_{\kappa=1}^{l}\big(\mathbf{u}^*\mathbf{b}\big)_\kappa w_\kappa\Big\}\, A_s, \tag{8.27}$$

where A_s is the area of the interior cell for $s = 1, \ldots, M$, w_κ are the weights used in the Gaussian quadrature for integrands with a logarithmic singularity, defined by $\int_0^1 \Big[\int_0^{1-\xi_2} f\,(\xi_1, \xi_2, \xi_3)\; d\xi\Big]\, d\xi_2 = \sum_{\kappa=1}^{n} w_\kappa\, f\,(\xi_1^\kappa, \xi_2^\kappa, \xi_3^\kappa)$, and ξ_1, ξ_2, ξ_3 are coordinates of the triangle (see Table A.12 on the CD-R for these nodes and weights).

We obtain a vector $\mathbf{B}_i$ as a result of the numerical integration of the body force terms by (8.27). In BE Eq (8.25) which corresponds to a node i the integral terms within the braces relate to node i with the element segment j over which the integrals are computed. Let us denote these integrals by $\hat{H}_{ij}$ and G_{ij} respectively, i.e.,

$$\hat{H}_{ij} = \int_{C_j} \mathbf{p}^*\, ds, \quad G_{ij} = \int_{C_j} \mathbf{u}^*\, ds,$$

each of which is a 2×2 matrix. Then Eq (8.25) becomes

$$\mathbf{c}(i)\mathbf{u}(i) + \sum_{j=1}^{N} H_{ij}\mathbf{u}_j = \mathbf{B}_i + \sum_{j=1}^{N} G_{ij}\mathbf{p}_j, \tag{8.28}$$

which relates the value of $\mathbf{u}$ at a mid-node i with the value of $\mathbf{u}$ and $\mathbf{p}$ at all the nodes j, including i. Let us write

$$H_{ij} = \begin{cases} \hat{H}_{ij} & \text{if } i \neq j \\ \hat{H}_{ij} + \mathbf{c}(i) & \text{if } i = j, \end{cases}$$

where $\mathbf{c}(i)$ is a coefficient matrix dependent on the boundary geometry, i.e.,

$$\mathbf{c}(i) = \begin{bmatrix} c(i) & 0 \\ 0 & c(i) \end{bmatrix},$$

and $c(i)$ is defined in (1.15). Hence, Eq (8.28) can be written as

$$\sum_{j=1}^{N} H_{ij}\mathbf{u}_j = \mathbf{B}_i + \sum_{j=1}^{N} G_{ij}\mathbf{p}_j, \tag{8.29a}$$

or in matrix form, as

$$HU = B + GP. \tag{8.29b}$$

Note that in Eq (8.29a) we know N_1 values of the displacements $\mathbf{u}_j$ and N_2 values of the tractions $\mathbf{p}_j$; thus, $2N - (N_1 + N_2)$ values are unknown in this equation. As we did in the case of potential problems (see (2.8)), we will collocate and rearrange Eq (8.29b) in the matrix form

$$AX = B + F, \tag{8.30}$$

where the unknowns are denoted by the vector X on the left side.

In Eq (8.29a), the integrals H_{ij} and G_{ij} are evaluated numerically by using the 4-point Gauss-Legendre quadrature formula except when $i = j$. The values of H_{ii} are easy to compute using rigid body considerations, but to compute G_{ij} we can use the logarithmic-Gauss integration formula, or for the two-dimensional isotropic case G_{ij} can also be evaluated analytically using (8.16) and Fig. 8.3.

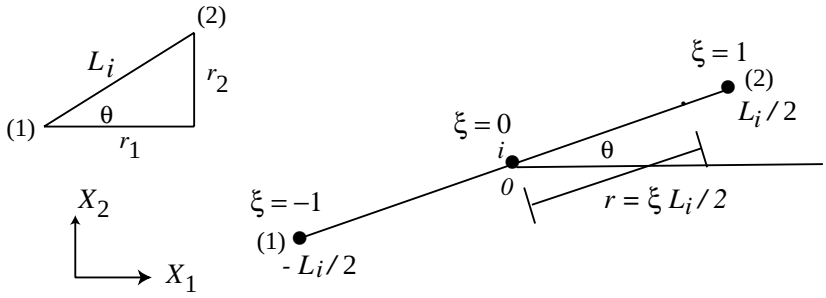

Fig. 8.3. Geometry at the node i.

Thus,

$$
\begin{aligned}
G_{11} &= \frac{1}{8\pi\mu(1-\nu)}\left[(3-4\nu)\int_{(1)}^{(2)}\ln\frac{1}{r}\,ds+\int_{(1)}^{(2)}\left(\frac{\partial r}{\partial x_1}\right)^2 ds\right]\\
&= \frac{1}{8\pi\mu(1-\nu)}\lim_{\varepsilon\to 0}\left[(3-4\nu)2\int_{\varepsilon}^{L_i/2}\ln\frac{1}{r}\,dr+2\int_{\varepsilon}^{L_i/2}\cos^2\theta\,dr\right]\\
&= \frac{1}{4\pi\mu(1-\nu)}\lim_{\varepsilon\to 0}\left[(3-4\nu)[r-r\ln r]_{\varepsilon}^{L_i/2}+\frac{r_1^2}{L_i^2}\left(\frac{L_i}{2}\right)\right]\\
&= \frac{L_i}{8\pi\mu(1-\nu)}\left[(3-4\nu)\left(1+\ln\frac{2}{L_i}\right)+\frac{r_1^2}{L_i^2}\right],\\
G_{12} &= \frac{1}{8\pi\mu(1-\nu)}\int_{(1)}^{(2)}\frac{\partial r}{\partial x_1}\frac{\partial r}{\partial x_2}\,ds\\
&= \frac{1}{8\pi\mu(1-\nu)}\lim_{\varepsilon\to 0}2\int_{\varepsilon}^{L_i/2}\sin\theta\cos\theta\,dr\\
&= \frac{1}{4\pi\mu(1-\nu)}\lim_{\varepsilon\to 0}2\int_{\varepsilon}^{L_i/2}\frac{r_1r_2}{L_i^2},dr=\frac{r_1r_2}{8\pi\mu(1-\nu)L_i}=G_{21},\\
G_{22} &= \frac{1}{8\pi\mu(1-\nu)}\left[(3-4\nu)\int_{(1)}^{(2)}\ln\frac{1}{r}\,ds+\int_{(1)}^{(2)}\left(\frac{\partial r}{\partial x_1}\right)^2 ds\right]\\
&= \frac{L_i}{8\pi\mu(1-\nu)}\left[(3-4\nu)\left(1+\ln\frac{2}{L_i}\right)+\frac{r_2^2}{L_i^2}\right],
\end{aligned}
$$

where L_i, as defined in (2.12), is the length of the element $\tilde{C}_i$. After solving (8.30), we use (8.25) and (8.27) to compute the displacements at an interior point as follows:

$$
\mathbf{u}(i)=\sum_{s=1}^{M}\Big\{\sum_{\kappa=1}^{l}\big(\mathbf{u}^*\mathbf{b}\big)_{\kappa}w_{\kappa}\Big\}A_s+\sum_{j=1}^{N}\Big\{\int_{C_j}\mathbf{u}^*\,ds\Big\}\mathbf{p}_j-\sum_{j=1}^{N}\Big\{\int_{C_j}\mathbf{p}^*\,ds\Big\}\mathbf{u}_j.
$$

The stress components at an interior point can be computed from (8.8), i.e.,

$$
\begin{aligned}
\sigma_{ij} &= \iint_R D_{ij}\mathbf{b}\,dx_1\,dx_2+\int_C D_{ij}\mathbf{p}\,ds-\int_C S_{ij}\mathbf{u}\,ds\\
&= \sum_{s=1}^{M}\Big\{\iint_{R_s}D_{ij}\,dx_1\,dx_2\Big\}\mathbf{b}_s+\sum_{j=1}^{N}\Big\{\int_{C_j}D_{ij}\,ds\Big\}\mathbf{p}_j-\sum_{j=1}^{N}\Big\{\int_{C_j}S_{ij}\,ds\Big\}\mathbf{u}_j,
\end{aligned}
$$

where

$$
D_{ij}=[D_1\ D_2],\quad S_{ij}=[S_1\ S_2],\quad \mathbf{p}=[p_1\ p_2]^T,\quad \mathbf{u}=[u_1\ u_2]^T,
$$

and for $k=1,2$,

$$
\begin{aligned}
D_k &= \frac{1}{4\pi(1-\nu)r}\Big[(1-2\nu)\big\{\delta_{ki}r_{,j}+\delta_{kj}r_{,i}-\delta_{ij}r_{,k}\big\}+2r_{.i}r_{,j}r_{,k}\Big],\\
S_k &= \frac{\mu}{2\pi(1-\nu)r^2}\Big[2\frac{\partial r}{\partial n}\big\{(1-2\nu)\delta_{ij}r_{,k}+\nu\big(\delta_{ik}r_{,j}+\delta_{jk}r_{,i}\big)-4r_{,i}r_{,j}r_{.k}\big\}\\
&\quad +2\nu\big(n_ir_{,j}r_{,k}+n_jr_{,i}r_{,k}\big)+(1-2\nu)\big(2n_kr_{,i}r_{,j}+n_j\delta_{ik}+n_i\delta_{jk}\big)-(1-4\nu)n_k\delta_{ij}\Big].
\end{aligned}
$$

Program Be11

We will develop this program for two-dimensional linear elastic boundary value problems for the case of constant elements of Fig. 2.2(a). The input file is created in the following order:

`N:` Number of boundary elements (same as the number of nodes in this case)

`L:` Number of interior points where results are to be computed

`M:` Number of different surfaces 1 through 5.

`Last:` Number of the last node on each different surface. Enter the last node numbers followed by zeros to a total of five entries

`mu:` shear modulus μ

`nu:` Poisson's ratio ν

`X, Y:` Coordinates of extreme points of the elements

`Xm, Ym:` Coordinates of the mid-nodes

`G:` Matrix defined in (8.29b)
After boundary conditions are applied, the matrix A of (8.26) is stored in this location.

`H:` Matrix defined in (8.29b)

`Code:` $= 0$ if displacements are prescribed,
$= 1$ if tractions are prescribed

`Bc:` Prescribed boundary conditions

`F:` Vector defined in (8.30)
After solution, the values of the unknowns are located here

`Xi, Yi:` Coordinates of the interior points

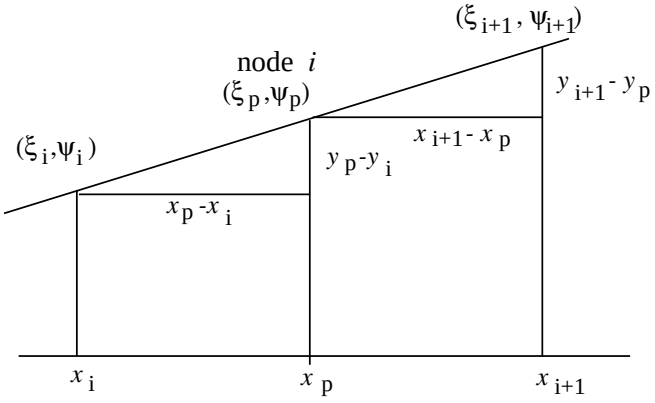

Fig. 8.4.

The output produces solution values of the displacement components at interior points (2 displacement values each point), and solution values of stresses $\sigma_x, \sigma_y, \tau_x y$ at interior points (3 stress values at each point). It can be seen from Fig. 8.4(a) that the equation of the boundary element with mid-node i is

$$m\,(x_i - x) - (y_i - y) = 0,$$

and thus,

$$\texttt{Perp} = \begin{cases} \big|m(x_i - x_p) - (y_i - y_p)\big|/\sqrt{1+m^2}, & \text{if } x_i \neq x_{i+1} \\ |x_i - x_p|, & \text{if } x_i = x_{i+1}. \end{cases}$$

From Fig. 8.4 it is easy to see that

$$\frac{y_{i+1} - y_p}{x_{i+1} - x_p} = \frac{y_p - y_i}{x_p - x_i}$$

which yields $(x_p - x_i)(y_{i+1} - y_p) - (x_{i+1} - x_p)(y_p - y_i) \equiv$ `sgn` (see (3.8) also). Note that `sgn` has the same sign as `slope` defined in §2.1, where other variables used in the program are also listed. This program calls the following functions: `Sys11, Quad11, Diag11, Inter11`, and `Solve`.

EXAMPLE 8.1. Consider the case of a circular hole under interior pressure embedded in an infinite medium, as shown in Fig. 8.5. The data is: $E = 94500$, $\nu = 0.1$. The input file is `ex8.1.in` and the output file is `ex8.1.out`. Note that the displacement (`Code`$= 0$) is prescribed zero at the nodes 16, 24, and 32 to keep the plate in equilibrium. Mathematically it means that the value of the constant for the displacement obtained as a result of integration is assumed to be zero. The solution for radial stress obtained from elasticity theory (see Timoshenko and Goodier 1951 pp. 78) is as follows:

Table 1.3.1

Point	Theoretical solution	BEM solution
$(4., 0.)$	-56.25	-56.8348
$(6., 0.)$	-25.0	-25.2413
$(10., 0.)$	-9.0	-9.0869
$(50., 0.)$	-0.36	-0.3635
$(200., 0.)$	-0.0225	-0.0227
$(1000., 0.)$	-0.0009	-0.0009

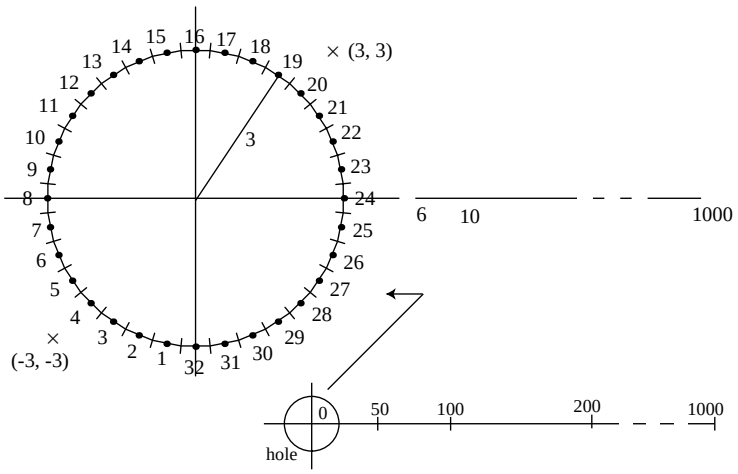

Fig. 8.5. Circular hole in an infinite medium.

The extreme points `X, Y` can be computed in the program, instead of being read, by using the formulas $x_j = 3\cos((j-1)\pi/16 + 17\pi/32)$, $y_j = -3\sin((j-1)\pi/16 + 17\pi/32)$, $j = 0, 1, \cdots, 32$ respectively. The boundary conditions at the nodes $j = 1, \ldots, 32$ are prescribed in order by the formulas

$$\texttt{Bc} \text{ in } x\text{-direction:} \quad 100\cos\left(\frac{j\pi}{16} + \frac{\pi}{2}\right),\ j = 0, 1, \ldots, 32,$$

$$\texttt{Bc} \text{ in } y\text{-direction:} \quad -100\sin\left(\frac{j\pi}{16} + \frac{\pi}{2}\right),\ j = 0, 1, \ldots, 32. \blacksquare$$

EXAMPLE 8.2. Consider the problem of a hollow circular pipe of radii $a = 10$ and $b = 15$ units respectively under an internal pressure $p = 100$ (see Fig. 8.6). The other data is: $\mu = 80,000$, and $\nu = 0.25$. Because of axial symmetry, the input file is created with constant elements as in Fig. 2.8(b). For the plane stress case, the displacements is given by

$$u(r) = \frac{pa^2}{E(b^2 - a^2}\left[(1-\nu)r + (1+\nu)\frac{b^2}{r^2}\right], \quad a \le r \le b,$$

and the stress by

$$\sigma(r) = \frac{pa^2}{E(b^2 - a^2)}\left(1 - \frac{b^2}{r^2}\right),$$

$$\theta(r) = \frac{pa^2}{E(b^2 - a^2)}\left(1 - \frac{b^2}{r^2}\right),$$

for $a \le r \le b$. Both circumferential and radial results for displacements and stresses compares very well with the exact solutions. However, the boundary element results for the stresses in the vicinity of the boundary do not match with the exact solutions; but this was expected. It is found that the boundary element results are, in general, correct for those interior points which lie at a distance more than half an element length away from the boundary.

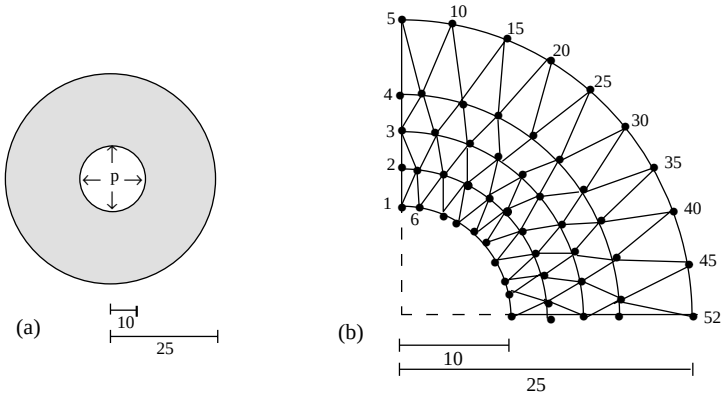

Fig. 8.6. A hollow circular pipe.

If this problem is solved with the finite element method of Fig. 8.6(b), with 52 nodes and 76 triangular elements, the results do not agree with the exact solutions. It means that if constant strains

are used in linear elasticity, the resulting finite elements computed at the center of each element will produce poor results. This method should therefore be avoided. ∎

9. README. The software required for BEM is provided on the enclosed CD-Rom. The programs are written in C, which is a case-sensitive structural language. The modules for each of the programs be1.c, be2.c, be5.c, and be11.c have the header `cbox1.h`, `cbox2.h`, `cbox5.h`, `cbox11.h` respectively, together with the C library headers ⟨`stdio.h`⟩ and ⟨`math.h`⟩. These modules can be compiled and linked separately for each program. Makefiles in each subdirectory will build the programs by simply typing 'make'.

There are two computation codes, one for UNIX and the other for DOS. The programs are run, e.g., for be1 as follows:

```
cd UNIX/BE1          or          > cd DOS\BE1
                    be1

FIRST LINE IN THE INPUT FILE SHOULD BE EITHER BLANK OR THE TITLE NOT DATA
Enter the name of the input file:EX5_1.IN
Enter the name of the output file:EX5_1.OUT
```

Other programs can be similarly run. UNIX C has been used to test run these programs on some benchmark problems using Sun WorkShop 6 update 2 C 5.3 on Solaris and gcc version 3.3.2 (Red Hat Linux $3.3.2-1$) on Linux. The DOS directory programs must be compiled and linked with the command appropriate for the system.

Note. If you have trouble running any one of these programs, note that the programs be1.c, be2.c, be5.c and be11.c were compiled with C compilers on a UNIX workstations. All these programs, and specially be11.c works perfectly well on UNIX SUN workstations and produces the same output as given in the above examples. Other C compiler(s) may give different results than those given above, or may fail to build the program.